

Generalized Polarizabilities of the proton

Nikos Sparveris

2nd Workshop on the Nucleon Structure at Low Q

Crete, May 2023

Outline

Introduction to the GPs

Overview: Experimental & Theoretical Status & Challenges

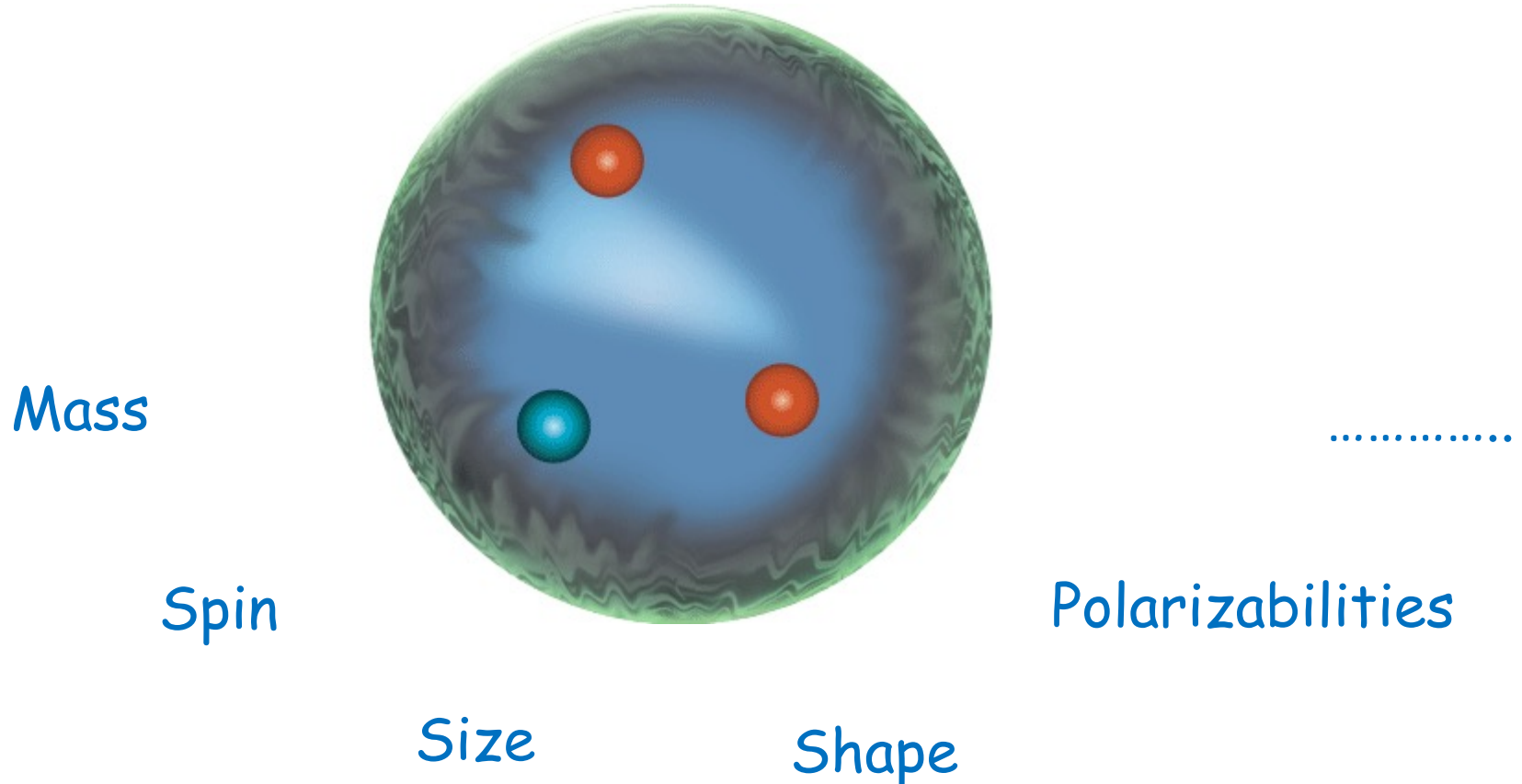
Recent results (Jlab / MAMI)

Prospects

Motivation

Explain how the proton emerges from the dynamics of the quark & gluon constituents

Measure and understand the emergence of the fundamental properties of the proton's bound state



Proton Polarizabilities

Fundamental structure constants
(such as mass, size, shape, ...)

Response of the nucleon to external EM field

Sensitive to the full excitation spectrum

Accessed experimentally through Compton Scattering

RCS: static polarizabilities \rightarrow net effect on the nucleon

Virtual Compton Scattering:

Virtuality of photon gives access to the GPs : $\alpha_E(Q^2)$ & $\beta_M(Q^2)$ (+ 4 spin GPs)

\rightarrow mapping out the spatial distribution of the polarization densities

Fourier transform of densities of electric charges and magnetization of a nucleon deformed by an applied EM field

PDG

150 Baryon Summary Table

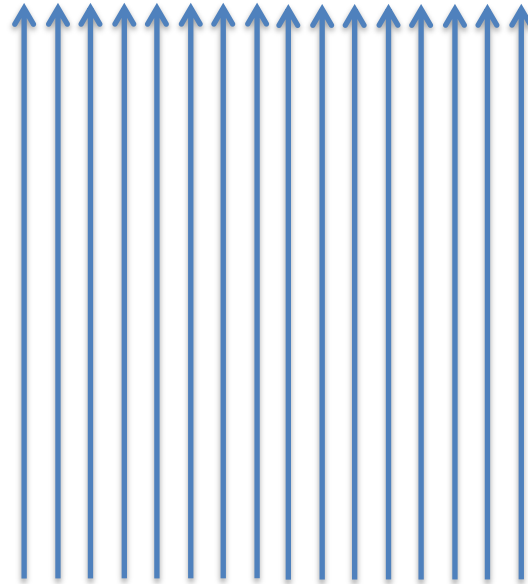
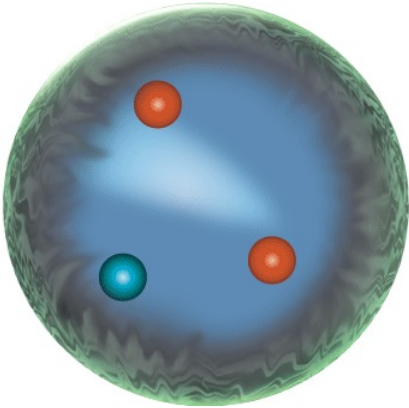
N BARYONS ($S = 0, I = 1/2$) $p, N^+ = uud; \quad n, N^0 = udd$	
---	--

p	$I(J^P) = \frac{1}{2}(\frac{1}{2}^+)$ Mass $m = 1.00727646681 \pm 0.00000000009 \text{ u}$ Mass $m = 938.272046 \pm 0.000021 \text{ MeV } [a]$ $ m_p - m_{\bar{p}} /m_p < 7 \times 10^{-10}, \text{ CL} = 90\% [b]$ $ q_p/m_p /(q_e/m_e) = 0.99999999991 \pm 0.00000000009$ $ q_p + q_{\bar{p}} /e < 7 \times 10^{-10}, \text{ CL} = 90\% [b]$ $ q_p + q_e /e < 1 \times 10^{-21} [c]$ Magnetic moment $\mu = 2.792847356 \pm 0.000000023 \mu_N$ $(\mu_p + \mu_{\bar{p}}) / \mu_p = (0 \pm 5) \times 10^{-6}$ Electric dipole moment $d < 0.54 \times 10^{-23} \text{ e cm}$ Electric polarizability $\alpha = (11.2 \pm 0.4) \times 10^{-4} \text{ fm}^3$ Magnetic polarizability $\beta = (2.5 \pm 0.4) \times 10^{-4} \text{ fm}^3 \quad (S = 1.2)$ Charge radius, μp Lamb shift $= 0.84087 \pm 0.00039 \text{ fm } [d]$ Charge radius, $e p$ CODATA value $= 0.8775 \pm 0.0051 \text{ fm } [d]$ Magnetic radius $= 0.777 \pm 0.016 \text{ fm}$ Mean life $\tau > 2.1 \times 10^{29} \text{ years}, \text{ CL} = 90\% [e] \quad (p \rightarrow \text{invisible mode})$ Mean life $\tau > 10^{31} \text{ to } 10^{33} \text{ years } [e] \quad (\text{mode dependent})$
----------	--

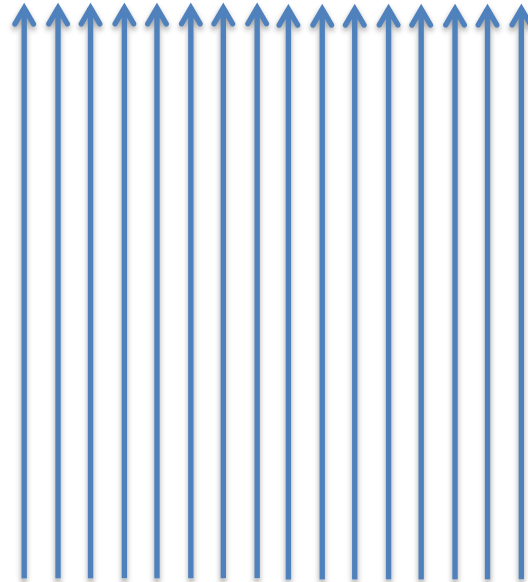
Scalar Polarizabilities

Response of internal structure to an applied EM field

Interaction of the EM field with the internal structure of the nucleon



\vec{E}

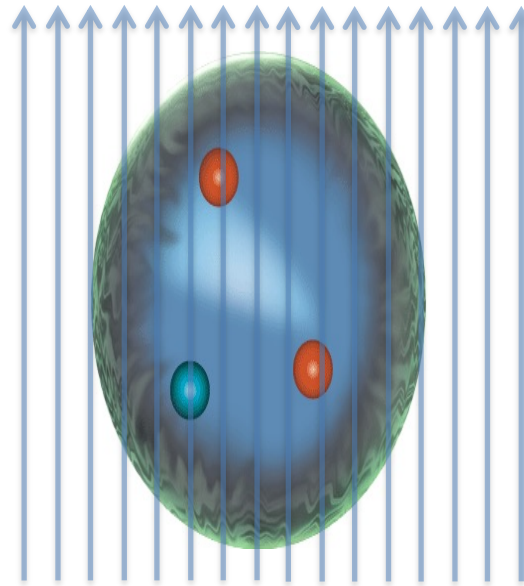
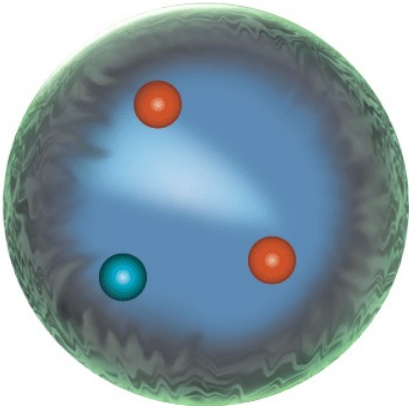


\vec{B}

Scalar Polarizabilities

Response of internal structure to an applied EM field

Interaction of the EM field with the internal structure of the nucleon

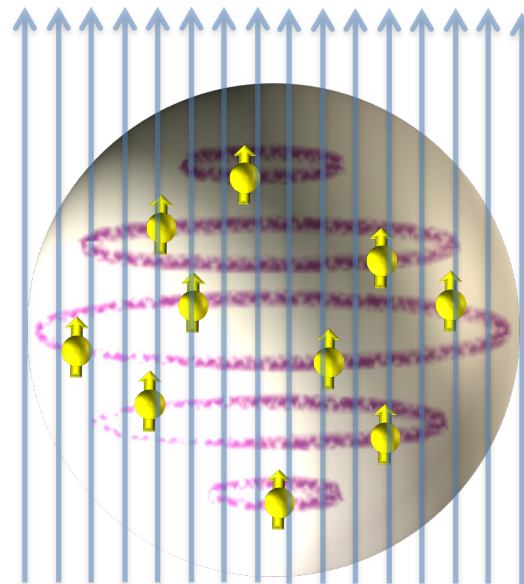


\vec{E}

“stretchability”

$$\vec{d}_{E \text{ induced}} \sim \alpha \vec{E}$$

External field deforms the charge distribution



\vec{B}

“alignability”

$$\vec{d}_{M \text{ induced}} \sim \beta \vec{B}$$

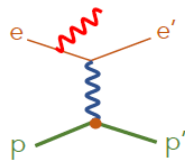
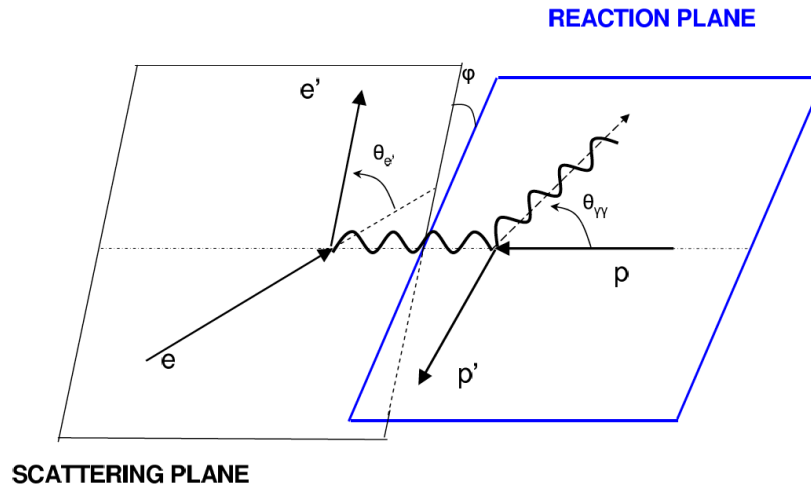
$$\beta_{\text{para}} > 0$$

$$\beta_{\text{diam}} < 0$$

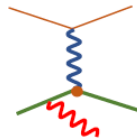
Paramagnetic: proton spin aligns with the external magnetic field

Diamagnetic: π -cloud induction produces field counter to the external perturbation

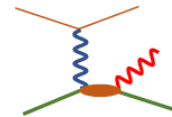
Virtual Compton Scattering



Bethe-Heitler



Born VCS



non-Born VCS

Elastic FFs

GPs

Virtual Compton Scattering

DR

valid below & above
Pion threshold

Dispersive integrals
for Non Born amplitudes

Spin GPs are fixed

Scalar GPs have
an unconstrained part

Fit to the experimental
cross sections at each Q^2

LEX

valid only below
Pion threshold

$$d^5\sigma = d^5\sigma^{BH+Born} + q'_{cm} \cdot \phi \cdot \Psi_0 + \mathcal{O}(q'^2_{cm})$$

$$\Psi_0 = v_1 \cdot (P_{LL} - \frac{1}{\epsilon} P_{TT}) + v_2 \cdot P_{LT}$$

Subtract the spin part

$$P_{TT} = [P_{TT \text{ spin}}]$$

$$P_{LT} = -\frac{2M}{\alpha_{em}} \sqrt{\frac{q'^2_{cm}}{Q^2}} \cdot G_E^p(Q^2) \cdot \beta_M(Q^2) + [P_{LT \text{ spin}}]$$

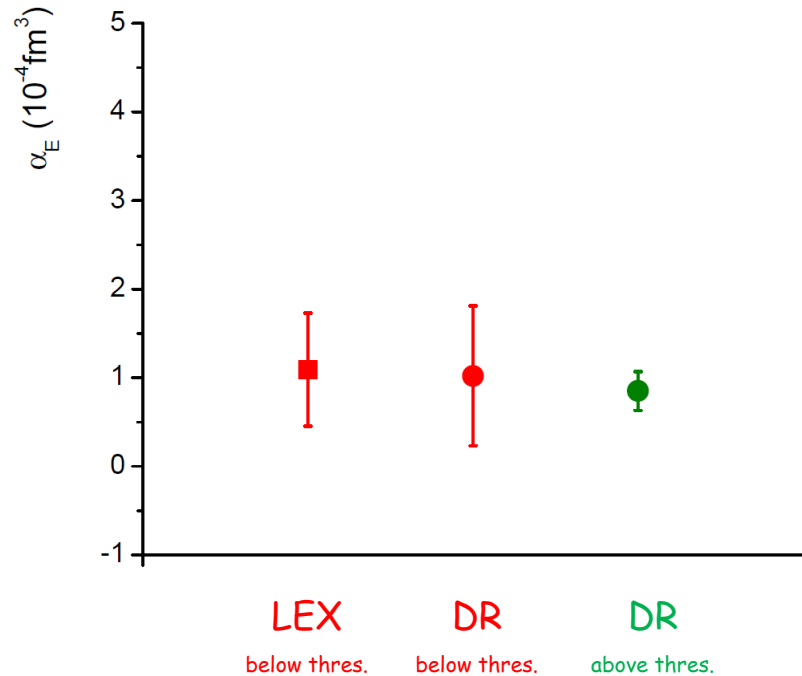
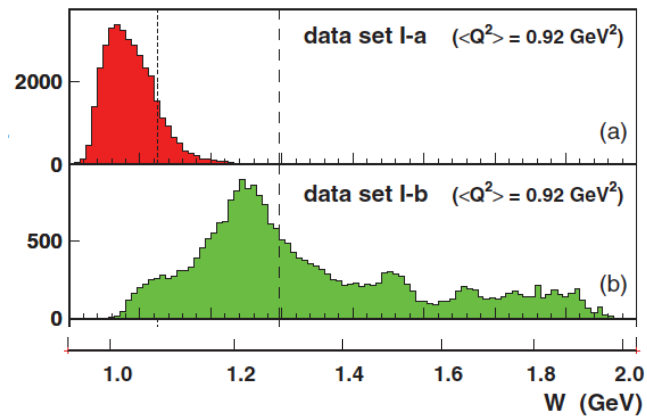
utilize DR

scalar GPs α_E and β_M

Virtual Compton Scattering

Phys. Rev C 86, 015210 (2012)

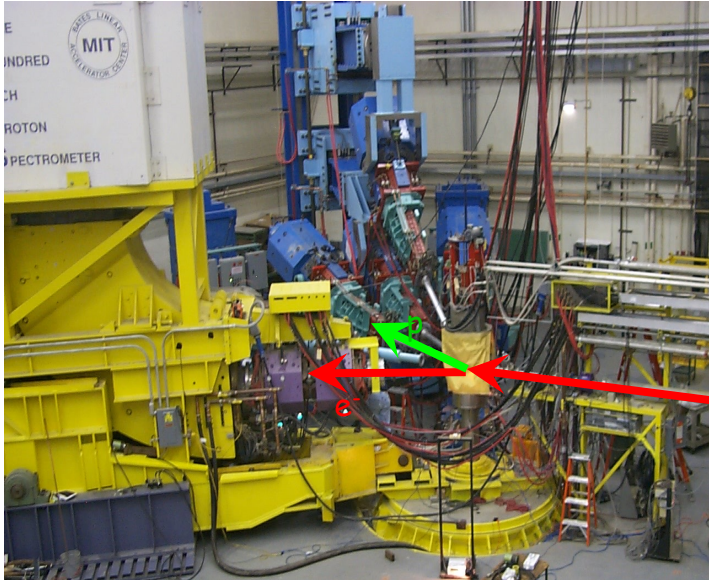
Phys. Rev Lett. 93, 122001 (2004)



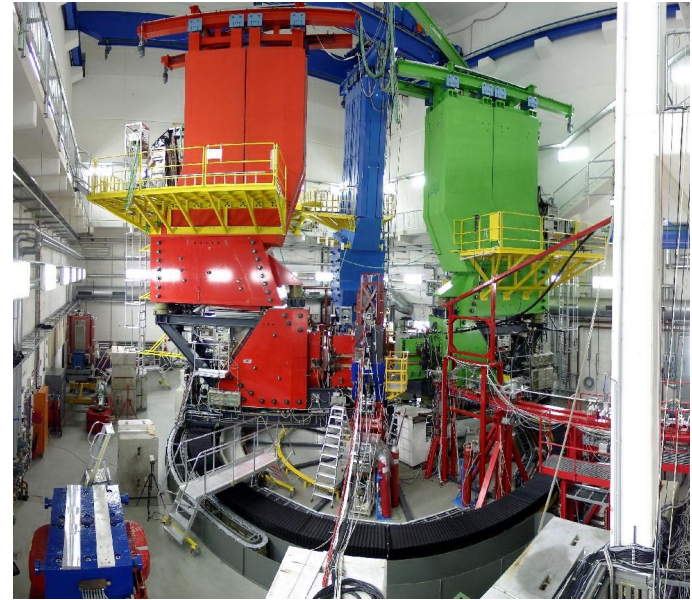
Sensitivity to the GPs grows as we measure above pion threshold

Early Experiments

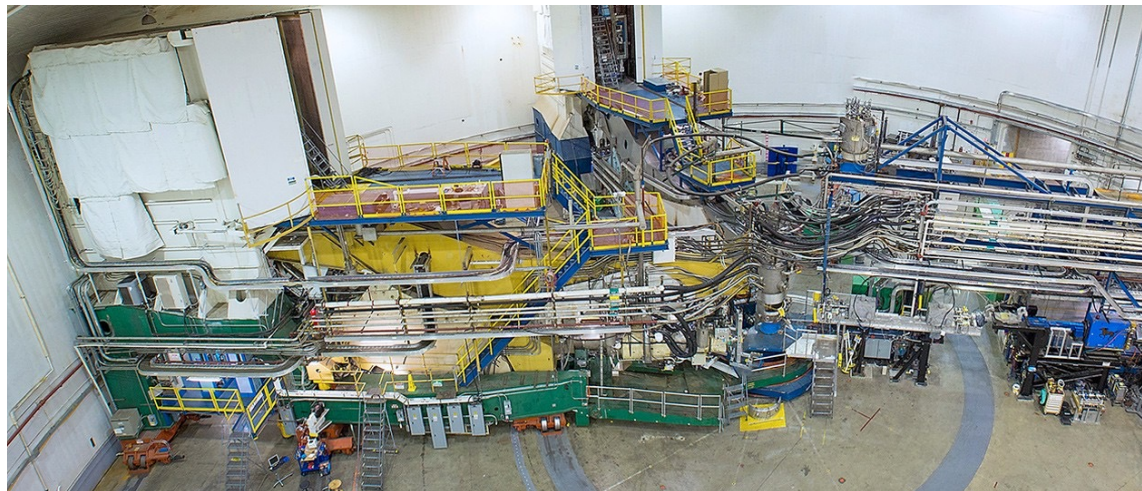
MIT-Bates @ $Q^2=0.06 \text{ GeV}^2$



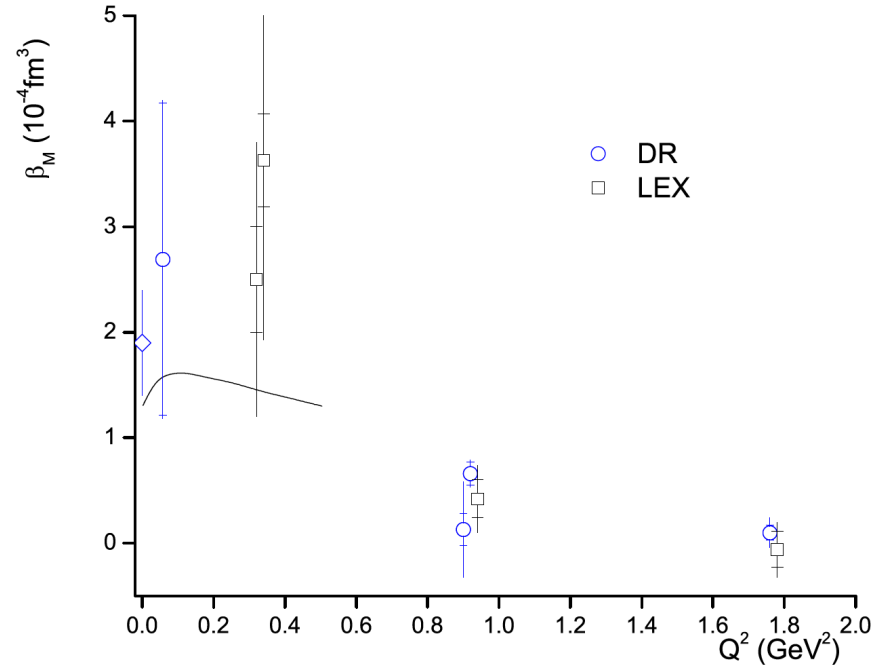
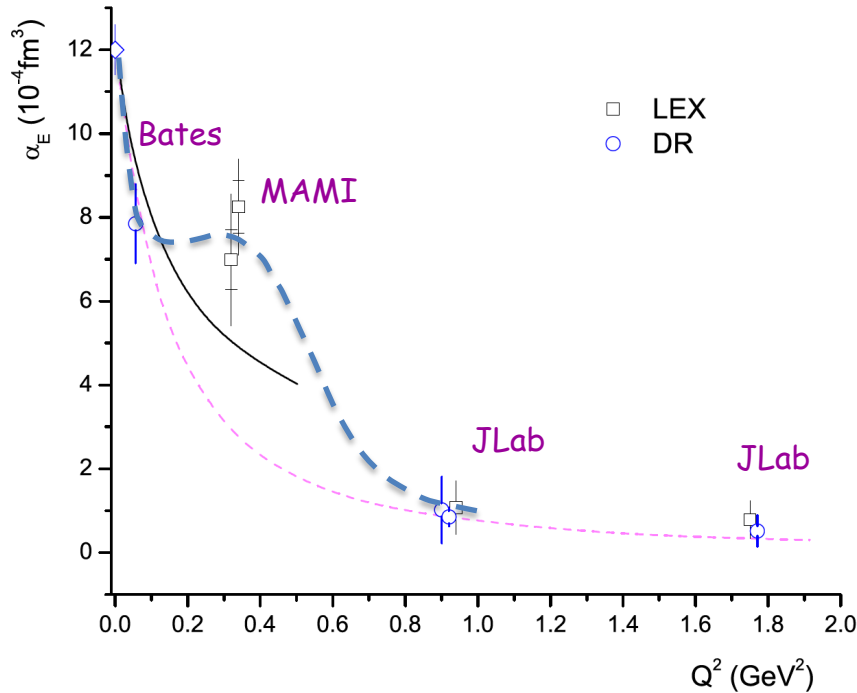
MAMI-A1 @ $Q^2=0.33 \text{ GeV}^2$



Jlab-Hall A @ $Q^2=0.9 \text{ \& } 1.8 \text{ GeV}^2$



Early Experiments



$\alpha_E \approx 10^{-3} V_N$ (stiffness / relativistic character)

Data: non-trivial Q^2 dependence of α_E (?)

Theory: monotonic fall-off

$Q^2 = 0.33 (\text{GeV}/c)^2$ measured twice at MAMI:

- Phys. Rev. Lett 85, 708 (2000)
- Eur. Phys. J. A37, 1-8 (2008)

β_M small \leftrightarrow cancellation of competing mechanisms

Large uncertainties

Higher precision measurements needed

→ Quantify the balance between diamagnetism and paramagnetism

Theory

HBChPT

NRQCM

Effective Lagrangian Model

Linear Sigma Model

T.R. Hemmert et al

B. Pasquini et al

A. Yu. Korchin and O. Scholten

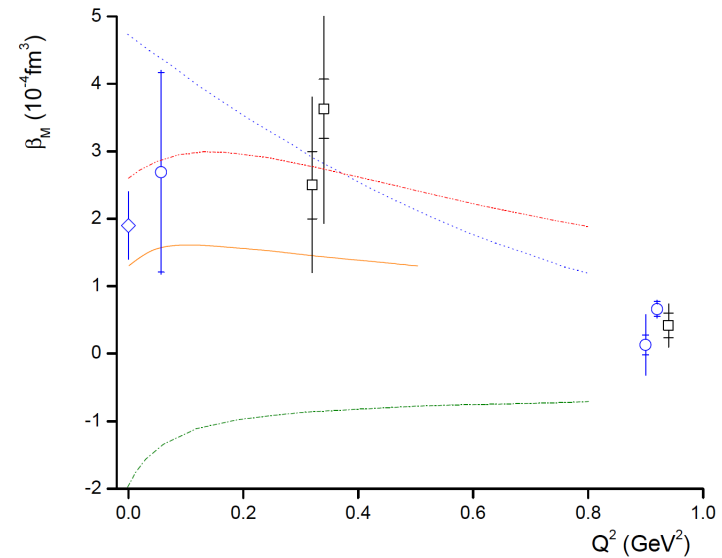
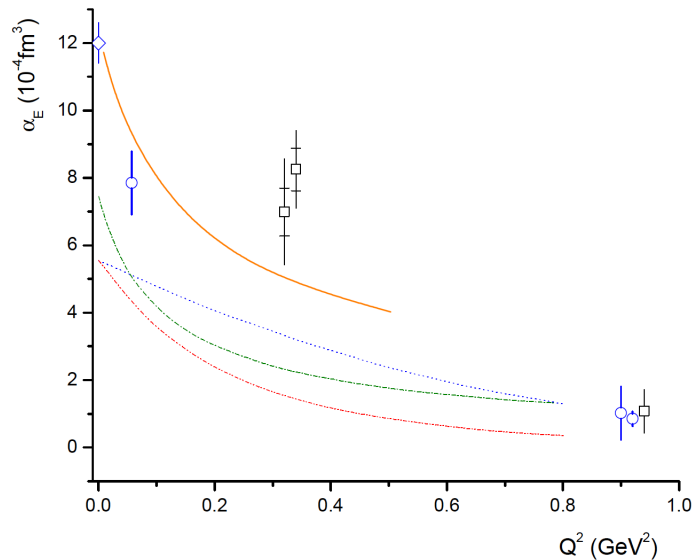
A. Metz and D. Drechsel

Phys. Rev. D 62, 014013 (2000)

Phys. Rev. C 63, 025205 (2001)

Phys. Rev. C 58, 1098 (1998)

Z. Phys. A 356, 351 (1996)



Smooth fall-off for α_E

A non-trivial structure for α_E is not supported by theory

Large spread in the predictions

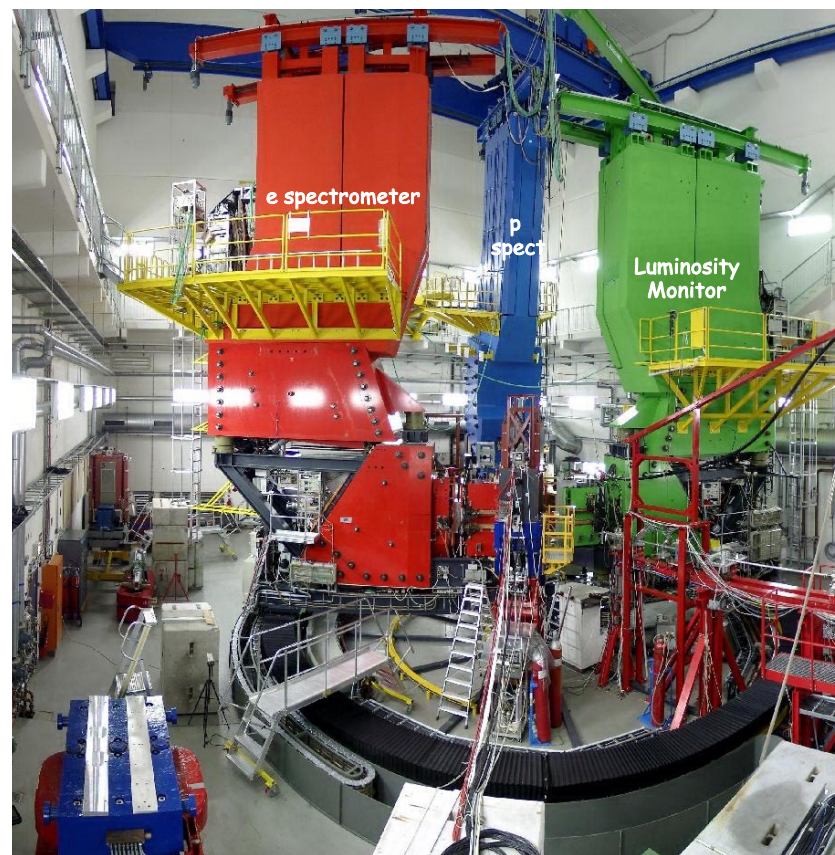
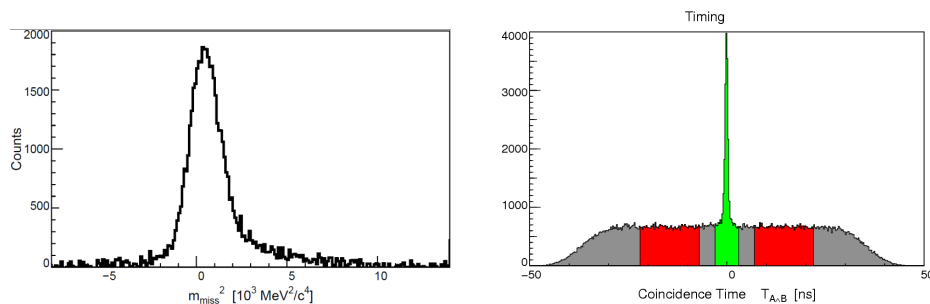
Recent Measurements

Recent Measurements: MAMI

MAMI A1/1-09 (vcsq2) below threshold

MAMI A1/3-12 (vcsdelta) above threshold

Both experiments utilized
the A1 setup at MAMI



For LEX the higher order terms have to be kept small / under control

$$d^5\sigma = d^5\sigma^{BH+Born} + q'_{cm} \cdot \phi \cdot \Psi_0 + \mathcal{O}(q'^2_{cm})$$

Refined analysis procedure / phase space masking to keep these terms smaller than $\sim 2\%$ - 3% level

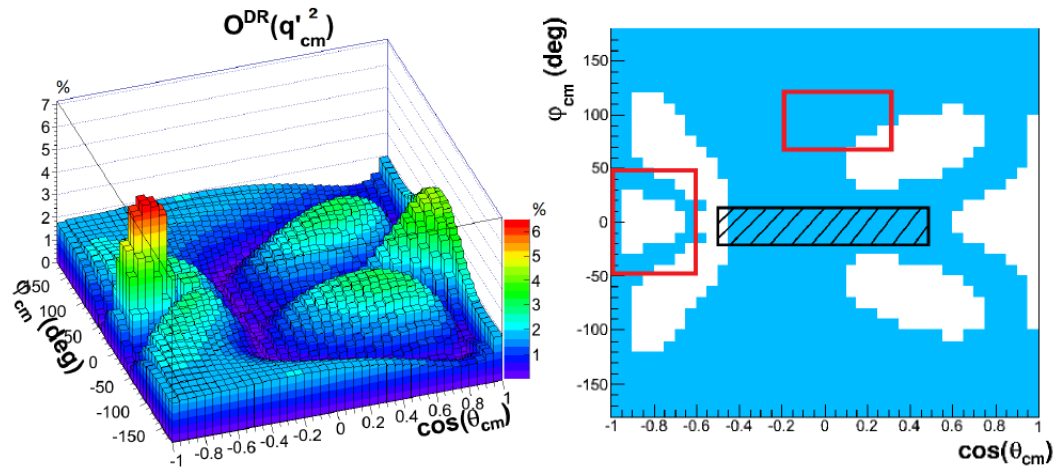
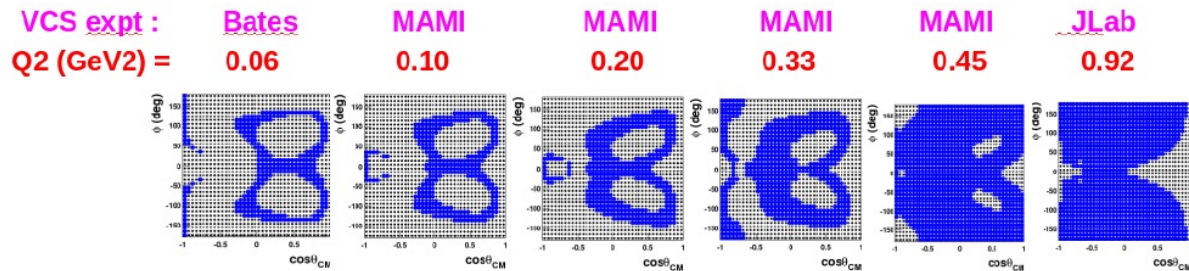
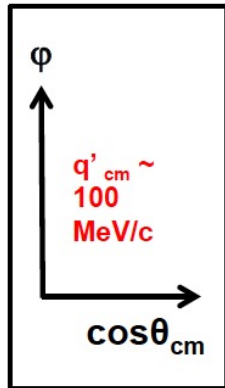


Figure 3.13: (Left) behavior of $\mathcal{O}^{DR}(q'^2_{cm})$ in the $(\cos(\theta_{cm}), \varphi_{cm})$ -plane at $q'_{cm} = 87.5 \text{ MeV}/c$ and (right) two-dimensional representation of the angular region where $\mathcal{O}^{DR}(q'^2_{cm}) < 2\%$ (blue), the red squares correspond to the two areas of interest to perform the GP extraction.

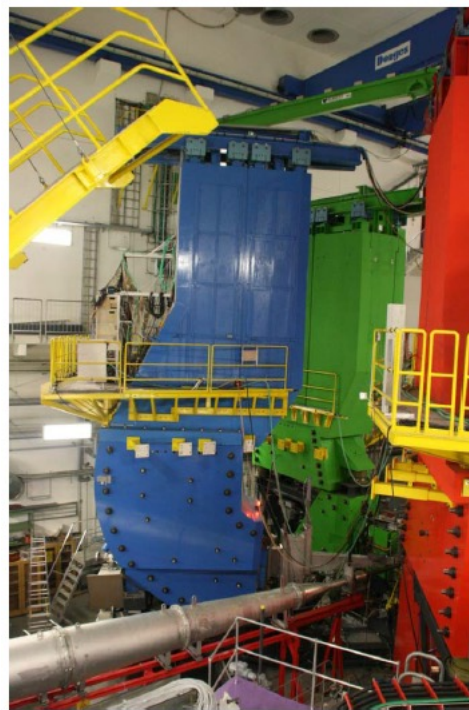
Figure from PhD thesis of L. Correa, Mainz / Cl. Ferrand

Blue bins = where the higher-order estimator is $< 3\%$
(LEX truncation « valid »)



New « vcsq2 » data:

- OOP kinematics (to access the blue region)
- LEX Fit done with bin selection at $Q^2 = 0.1$ and 0.2 GeV^2 .
- was found not necessary at $Q^2 = 0.45 \text{ GeV}^2$.



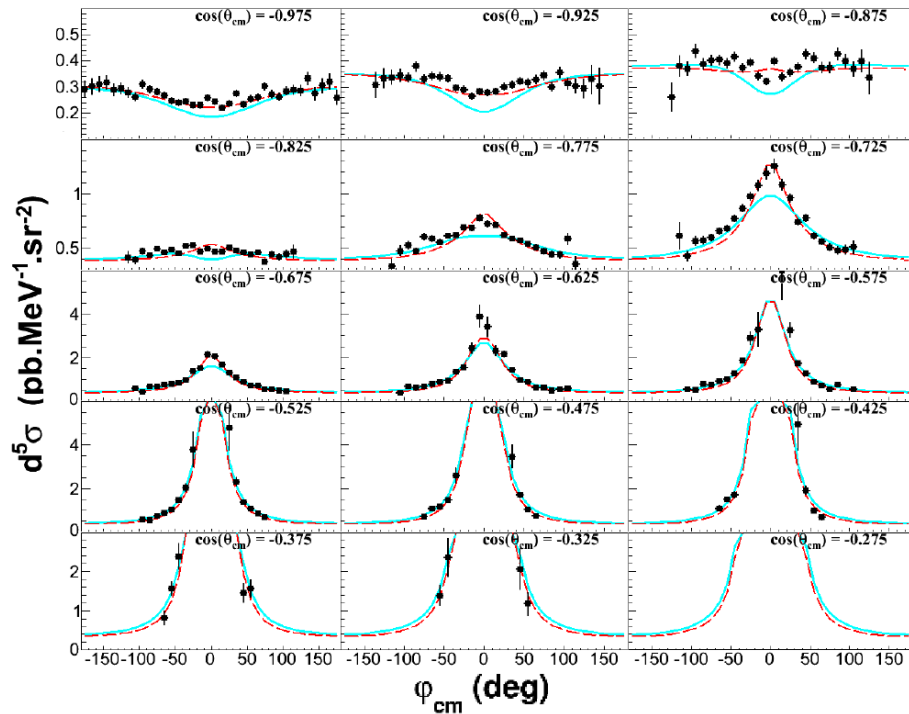
In-plane



8.5 deg OOP

~ 1.0 GeV beam

$Q^2 = 0.1 \text{ (GeV/c)}^2, 0.2 \text{ (GeV/c)}^2, \text{ and } 0.45 \text{ (GeV/c)}^2$



BH+B ---
Polarizability effect ---

GP effect typically 5% - 15% of the cross section

Polarizability fits:

DR fit:
DR calculation includes full dependency in q'_{cm}

LEX fit:
truncated in q'_{cm} . Suppress contribution from higher order terms

Figure 5.8: Setting INP: measured $ep \rightarrow ep\gamma$ cross section at fixed $q'_{cm} = 112.5 \text{ MeV/c}$ with respect to φ_{cm} for all the $\cos(\theta_{cm})$ -bins. The curves follow the convention of figure 5.6.

A1/3-12 @ MAMI

- Goal 2-fold:
- 1) Measure α_E
 - 2) First measurement of $N \rightarrow \Delta$ transition form factors through the γ channel

1.1 GeV beam, 5cm LH₂

A1 spectrometers A & B in coinc.

$$Q^2 = 0.2 \text{ (GeV/c)}^2$$

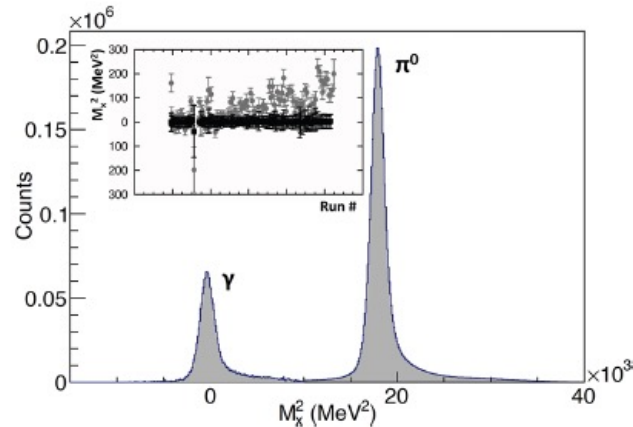
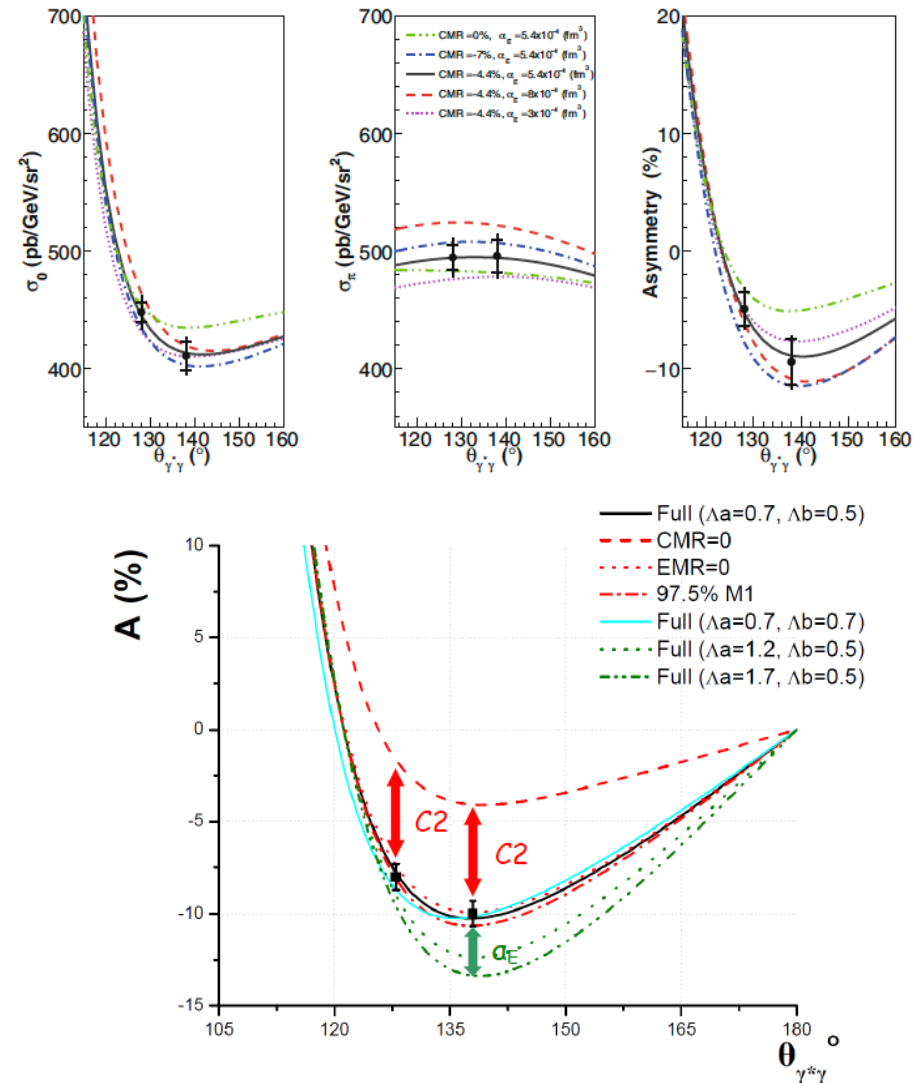


Fig. 1. The missing mass spectrum. The two peaks corresponding to the photon and to the π^0 are very well separated. The photon peak has been multiplied by a factor of 10 so that it can be clearly seen in the figure. The inserted panel shows the center of the photon missing mass peak before (gray circle) and after (black box) the momentum calibration as a function of the different run numbers.



MAMI Results

Phys. Rev. Lett 123, 192302

Phys. Rev. C 103, 025205

Eur. Phys. J. A55, 182

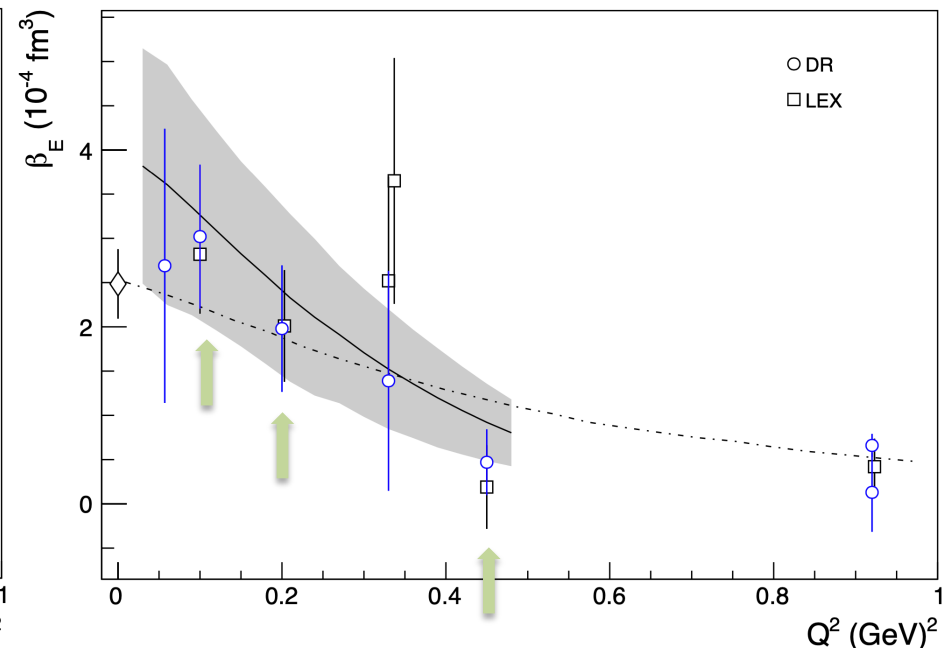
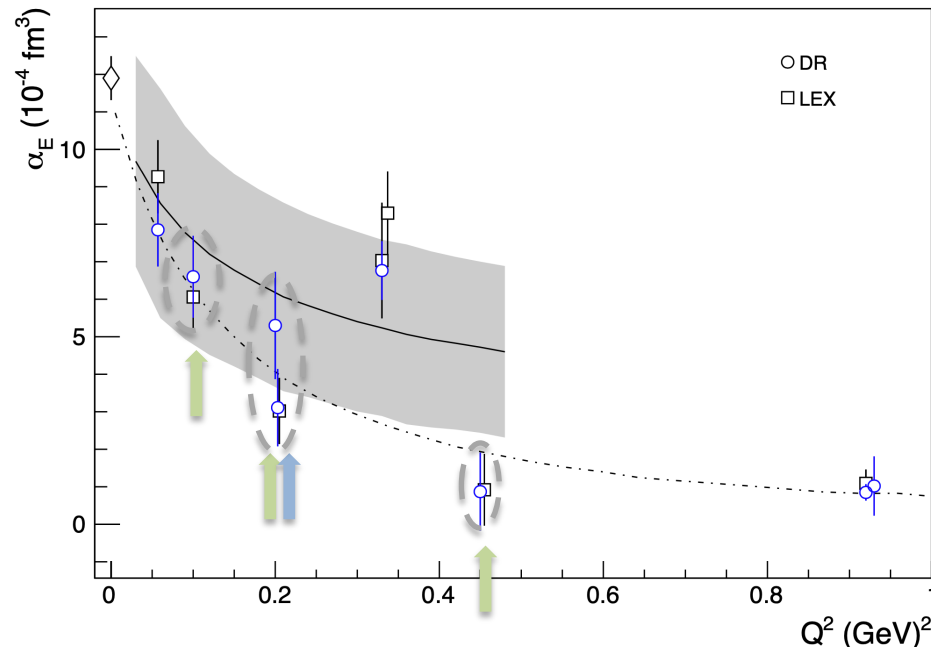
PhD students:

Jure Bericic (Ljubljana Univ.)

Loup Correa (Clermont-Fd Univ.)

Meriem BenAli (Clermont-Fd Univ.)

Adam Blomberg (Temple Univ.)



A1/1-09 @ MAMI

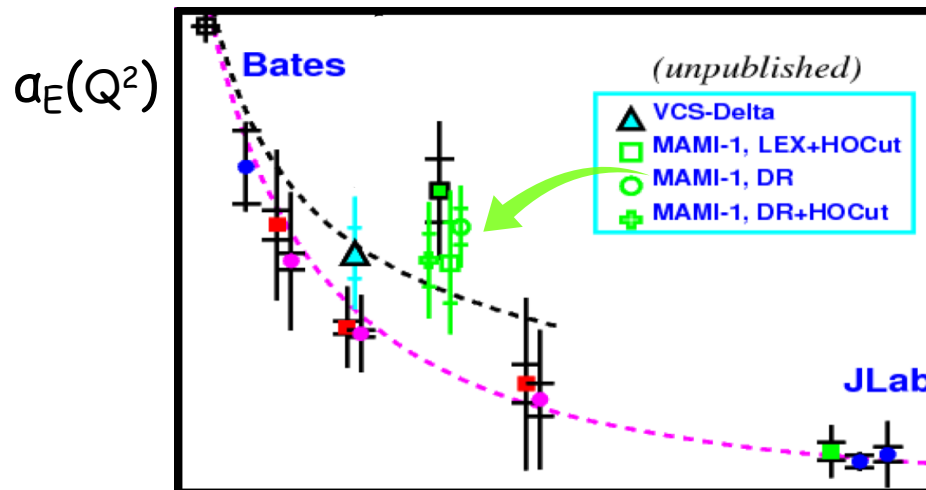
A1/3-12 @ MAMI

Revisiting the $Q^2=0.33 \text{ GeV}^2$ data

$Q^2 = 0.33 \text{ (GeV/c)}^2$ measured twice at MAMI - two different experiments

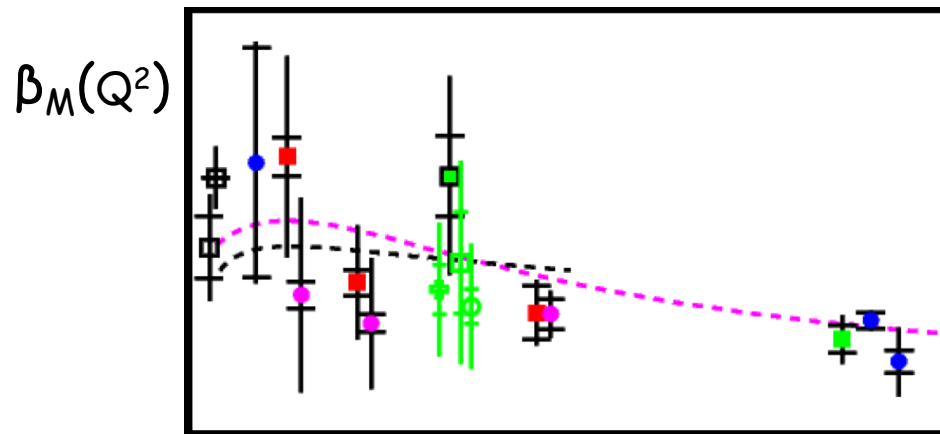
- Phys. Rev. Lett 85, 708 (2000)
- Eur. Phys. J. A37, 1-8 (2008)

Analysis revisited (unpublished):



Re-fits at
 $Q^2=0.33$
 GeV^2
(H.F.)

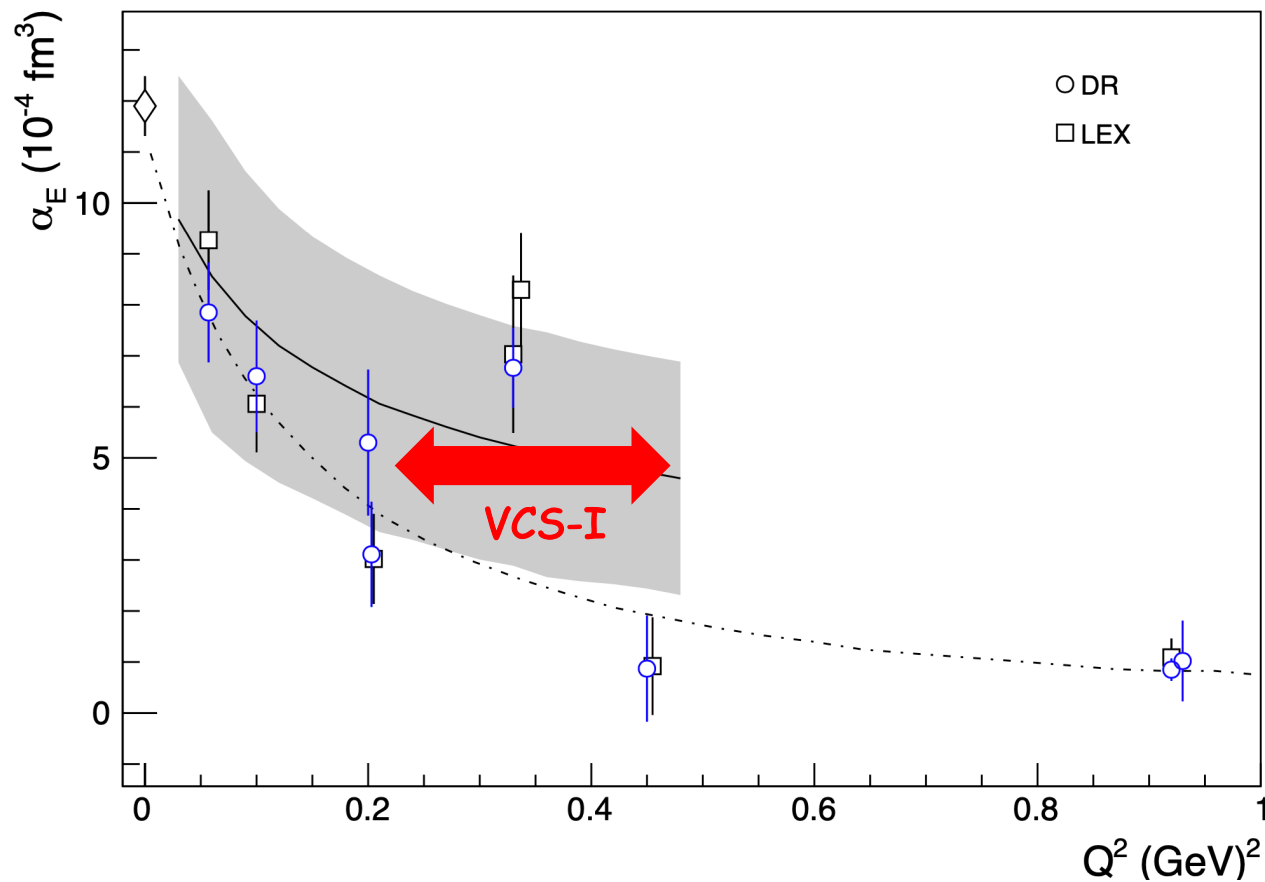
LEX and DR
Updated HO-cut



The a_E puzzle still holds

Jlab : Experiment E12-15-001 (VCS-I) in Hall C

High precision measurements targeting explicitly the kinematics of interest for a_E



Hall C HMS and SHMS

SHMS:

- 11-GeV Spectrometer
- Partner of existing 6-GeV HMS

MAGNETIC OPTICS:

- Point-to Point QQQD for easy calibration and wide acceptance.
- Horizontal bend magnet allows acceptance at forward angles (5.5°)

Detector Package:

- Drift Chambers
- Hodoscopes
- Cerenkovs
- Calorimeter
- All derived from existing HMS/SOS detector designs

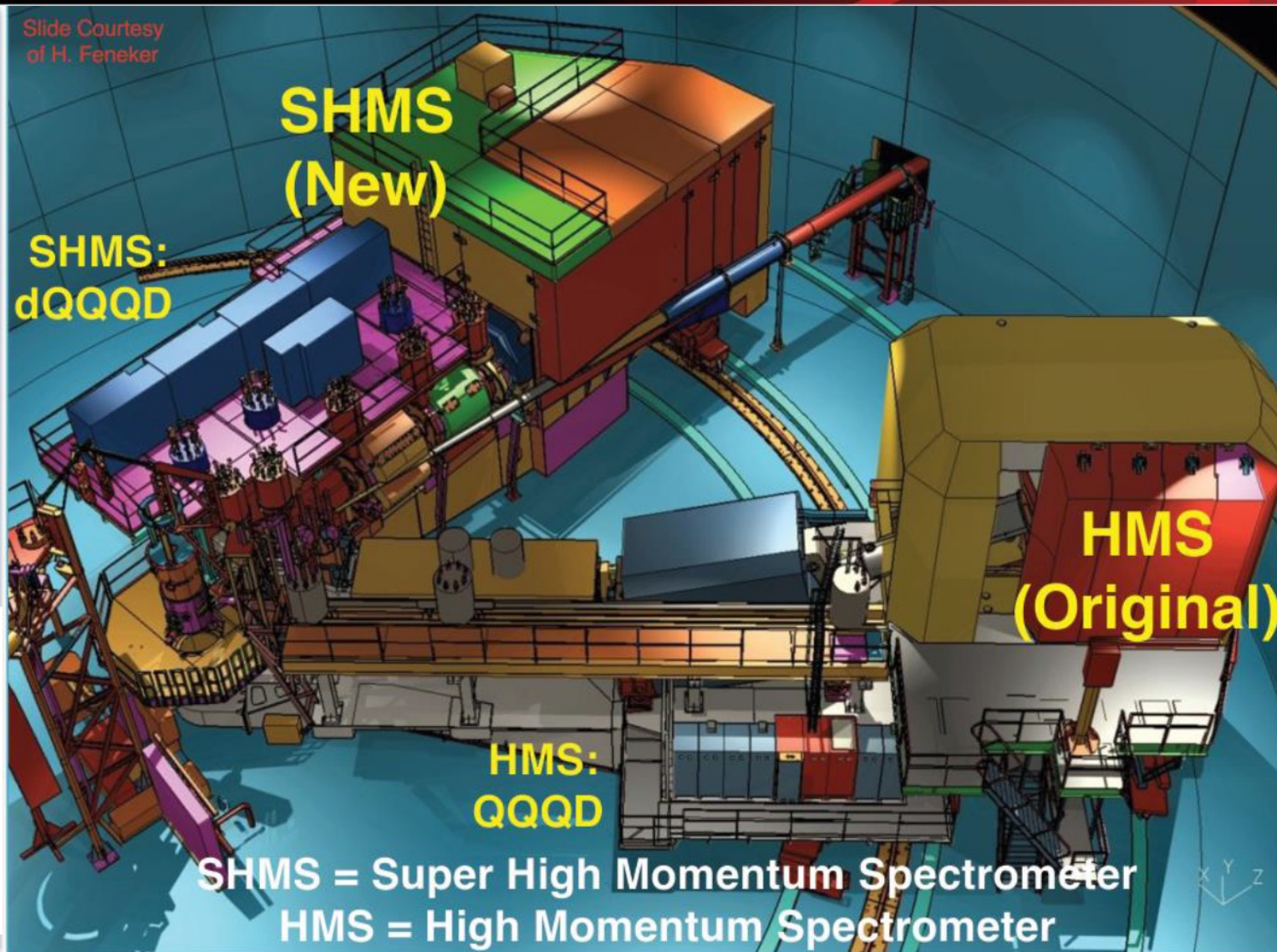
• Super High Momentum Spectrometer

- HB, 3 Quads, Dipole
- $P \rightarrow 2 - 11 \text{ GeV}$
- Resolution: $\delta < 0.1\%$
- Acceptance: $\delta \rightarrow 30\%$, 4 msr
- $5.5^\circ < \theta < 40^\circ$
- Good $e/\pi/K/p$ PID

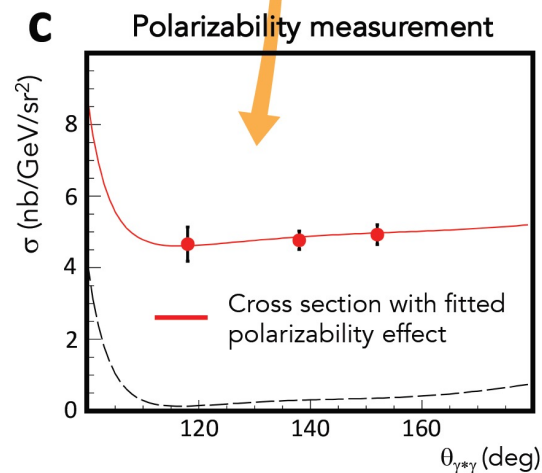
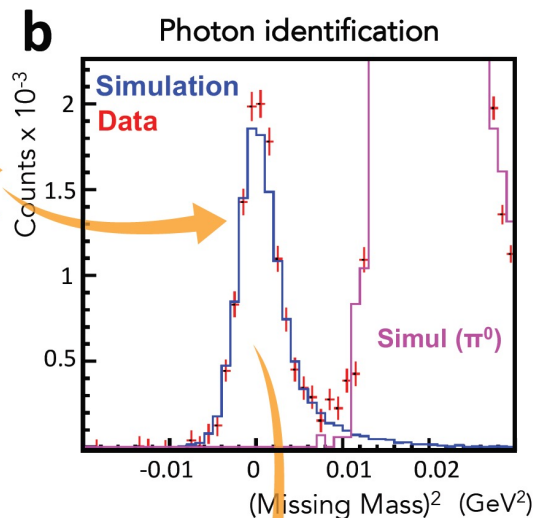
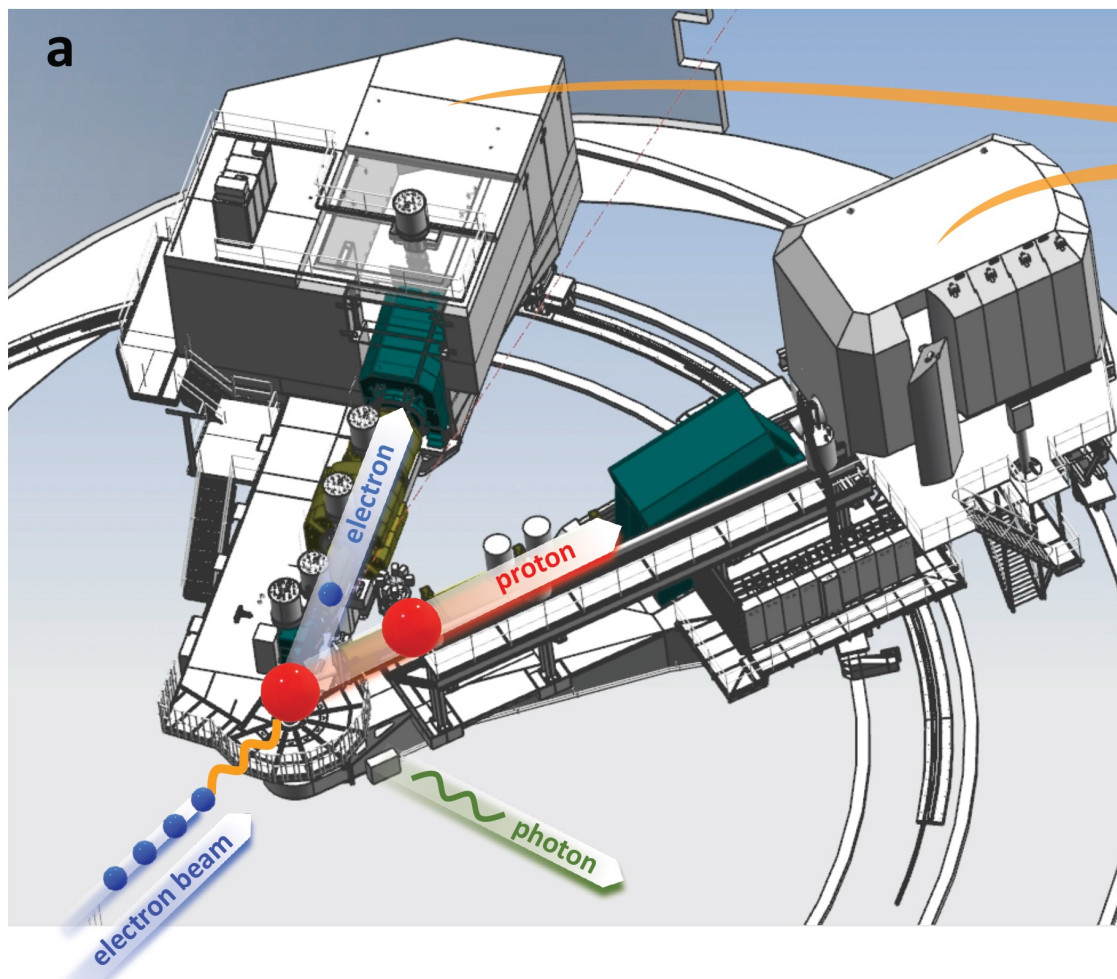
• High Momentum Spectrometer

- 3 Quads, Dipole
- $P \rightarrow 7.5 \text{ GeV}$
- Resolution: $\delta < 0.1\%$
- Acceptance: $\delta \rightarrow 18\%$, 6.5 msr
- $10.5^\circ < \theta < 90^\circ$
- Good $e/\pi/K/p$ PID

Slide Courtesy
of H. Feneker



The experiment



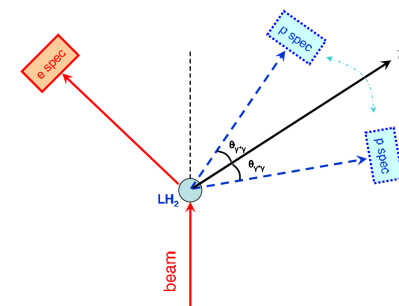
Hall C: SHMS, HMS
4.56 GeV
20 μ A
Liquid hydrogen 10 cm

cross sections & azimuthal asymmetries

$$A_{(\phi_{\gamma^*\gamma}=0,\pi)} = \frac{\sigma_{\phi_{\gamma^*\gamma}=0} - \sigma_{\phi_{\gamma^*\gamma}=180}}{\sigma_{\phi_{\gamma^*\gamma}=0} + \sigma_{\phi_{\gamma^*\gamma}=180}}$$

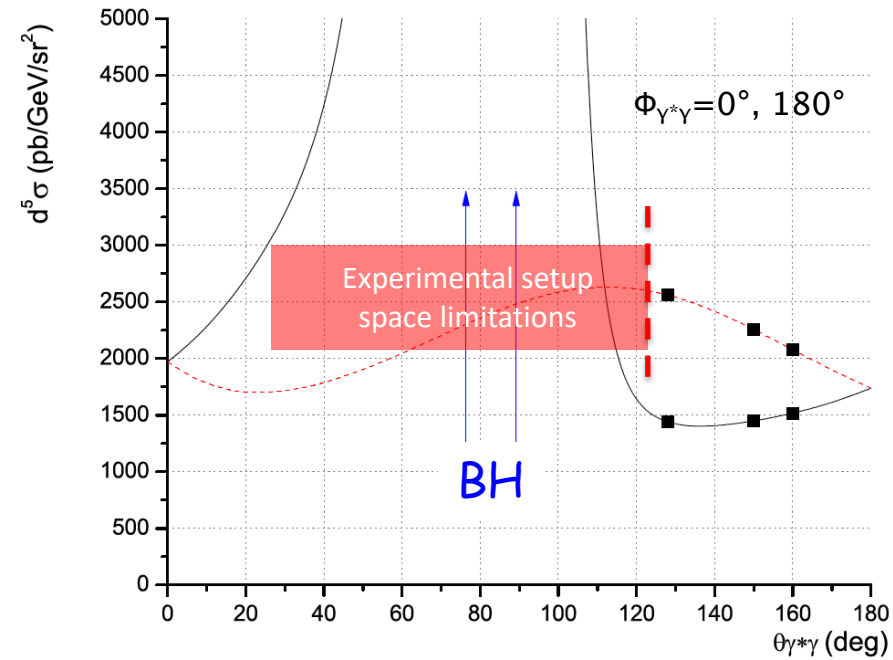
sensitivity to GPs

suppression of systematic asymmetries

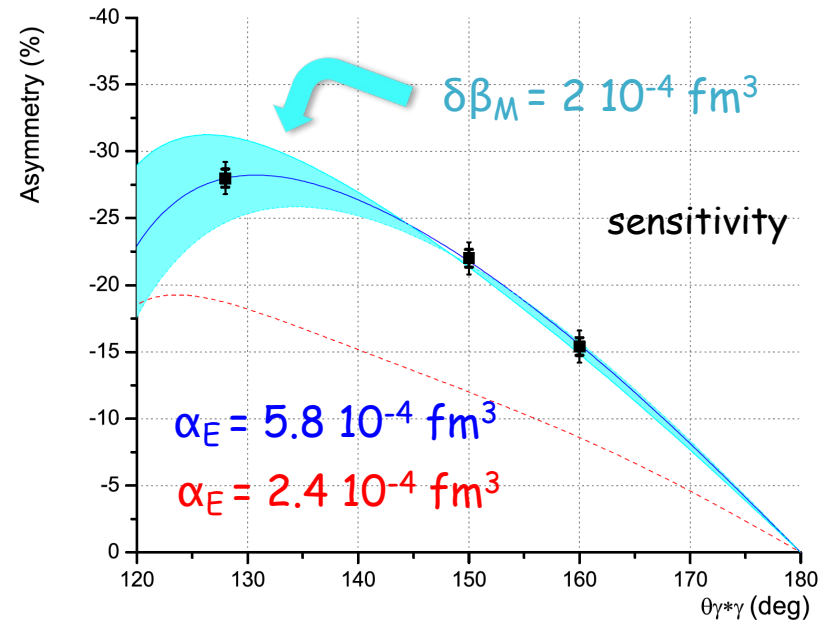


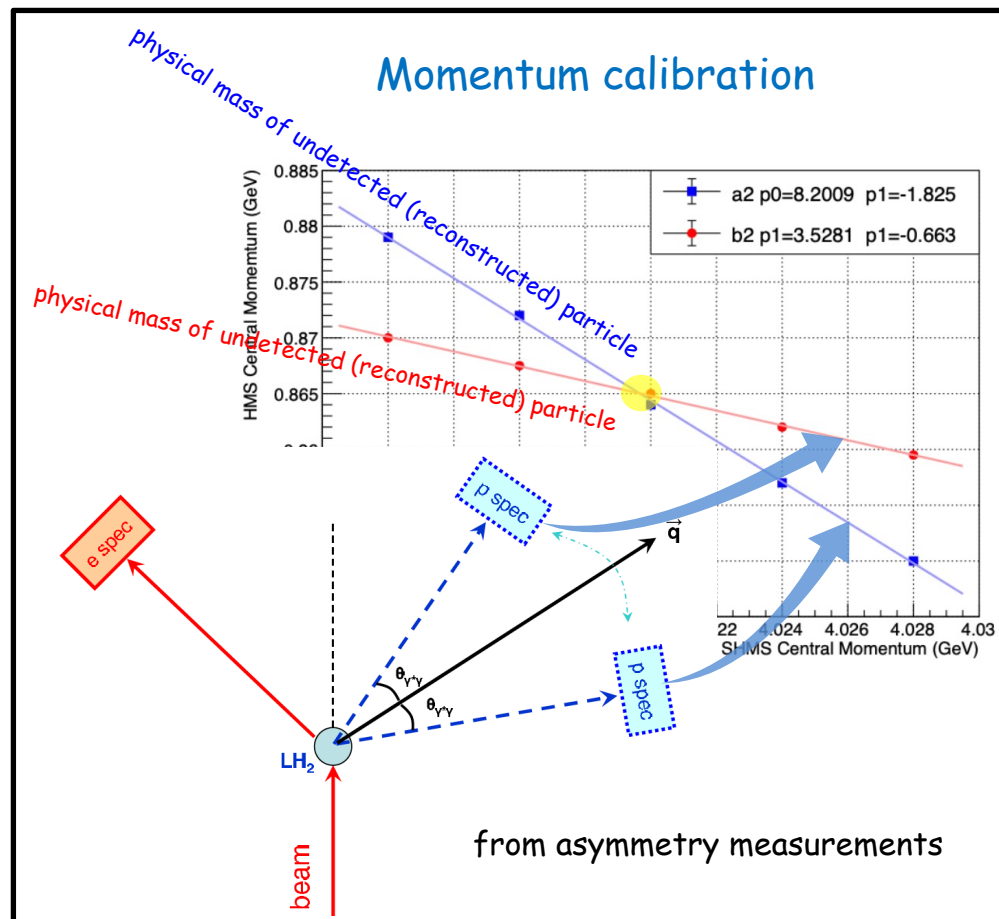
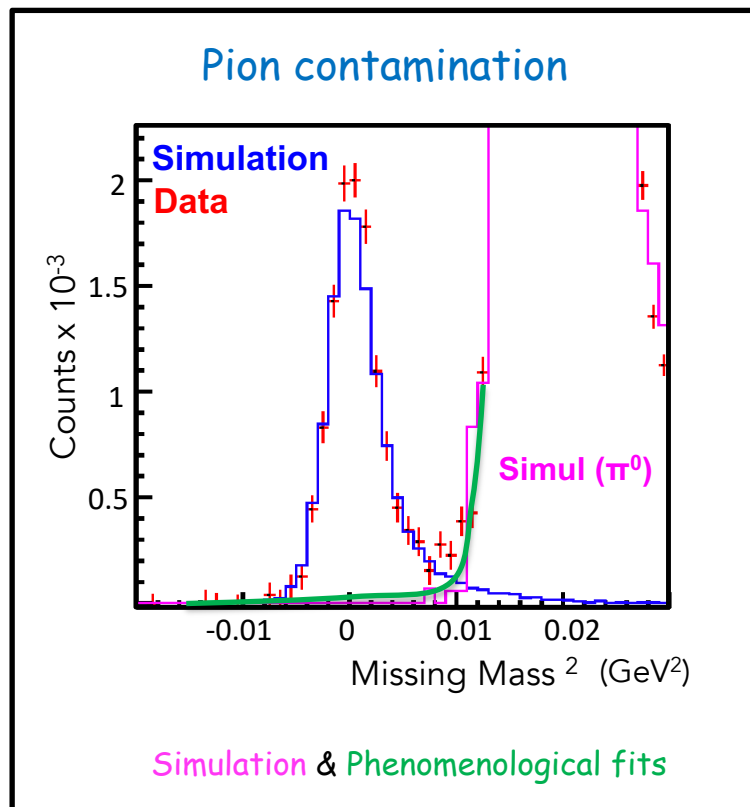
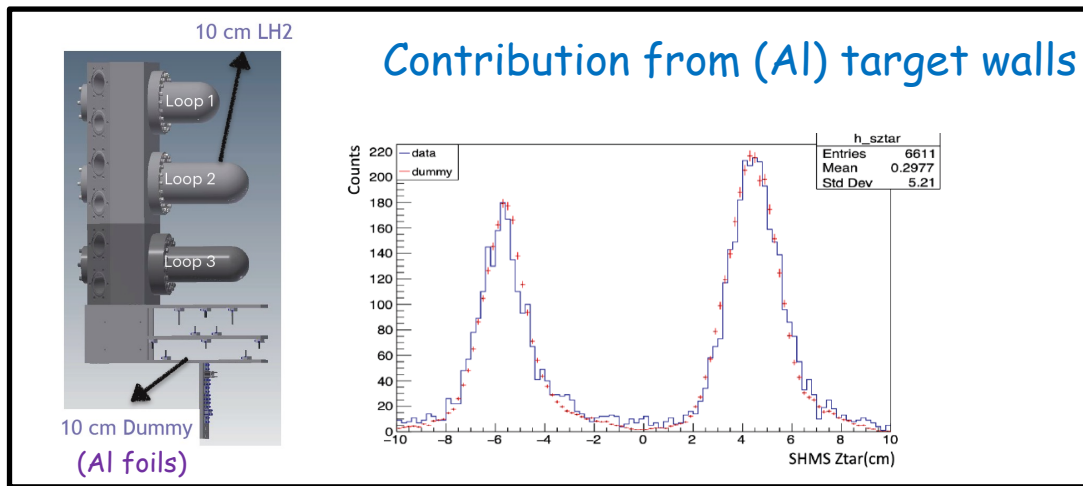
Kinematics

$$Q^2 = 0.4 \text{ (GeV/c)}^2$$



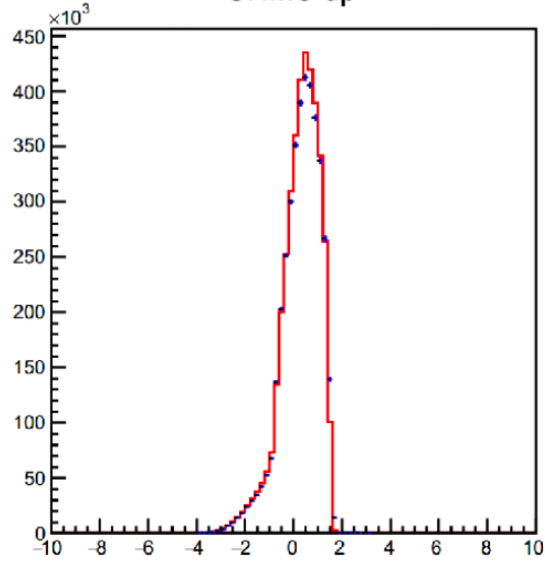
avoid BH region ($\theta_{\gamma^*\gamma} > 120^\circ$)



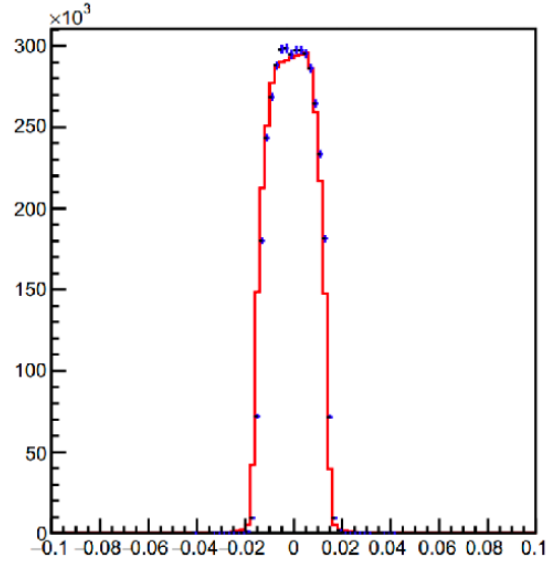


Elastic data

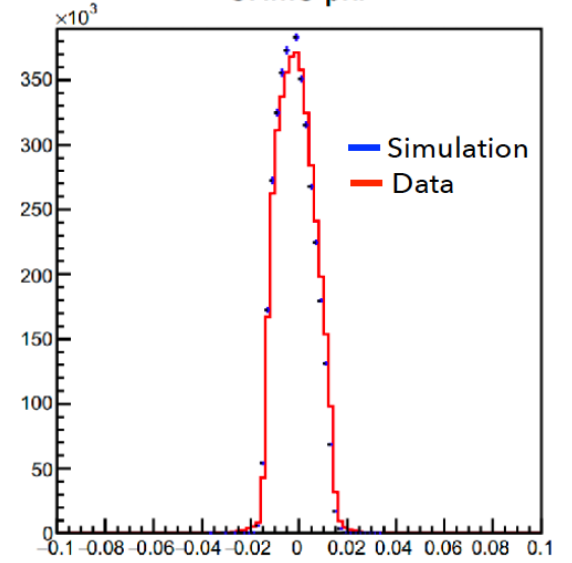
SHMS dp



SHMS theta

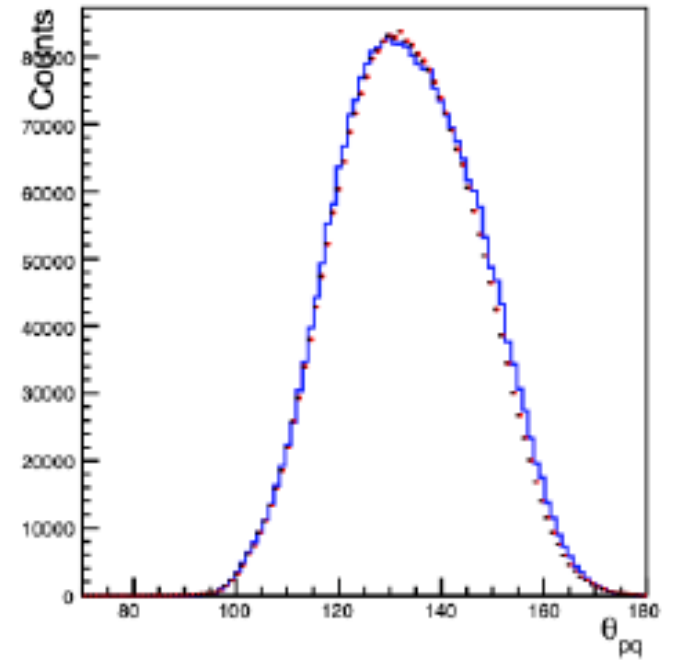
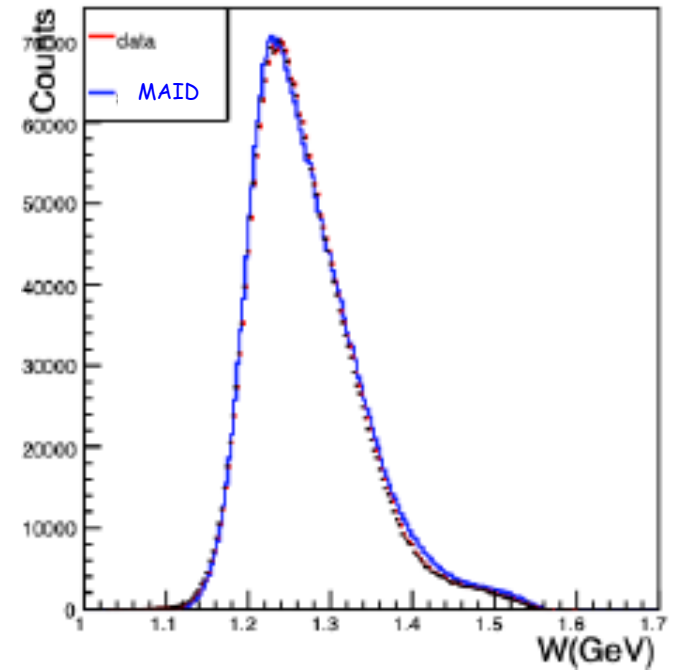
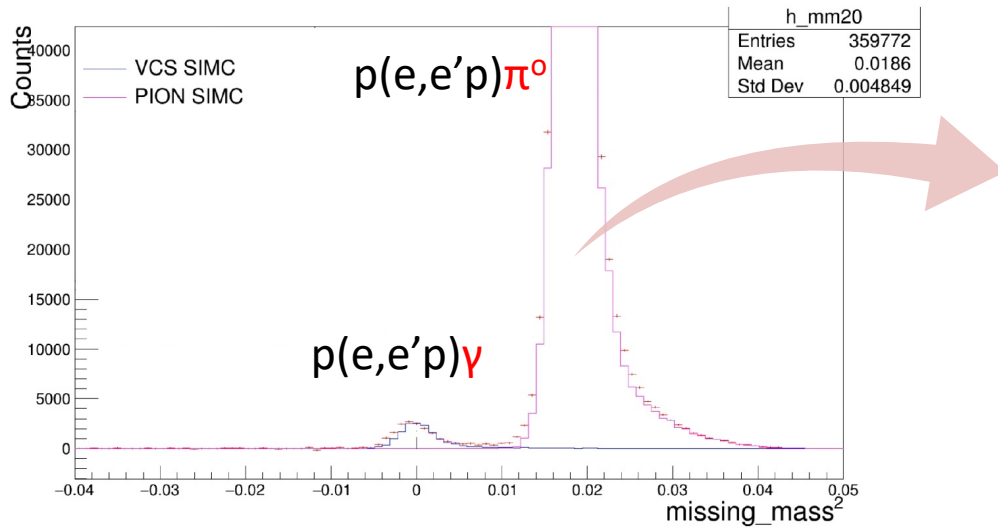


SHMS phi

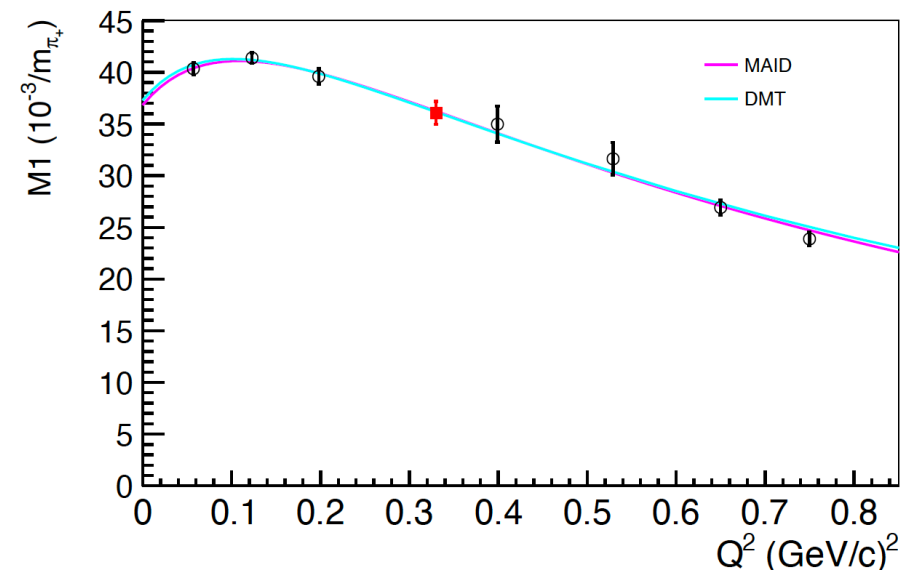
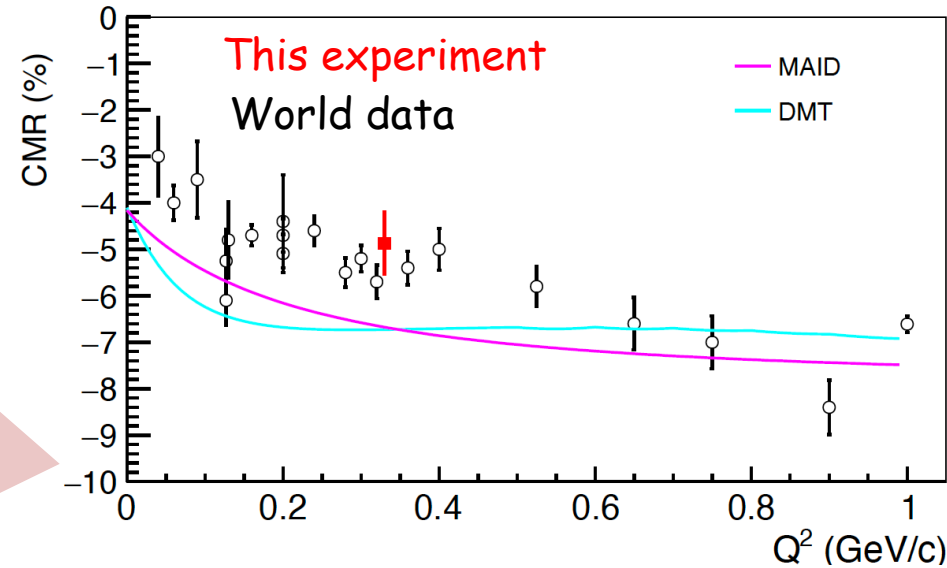
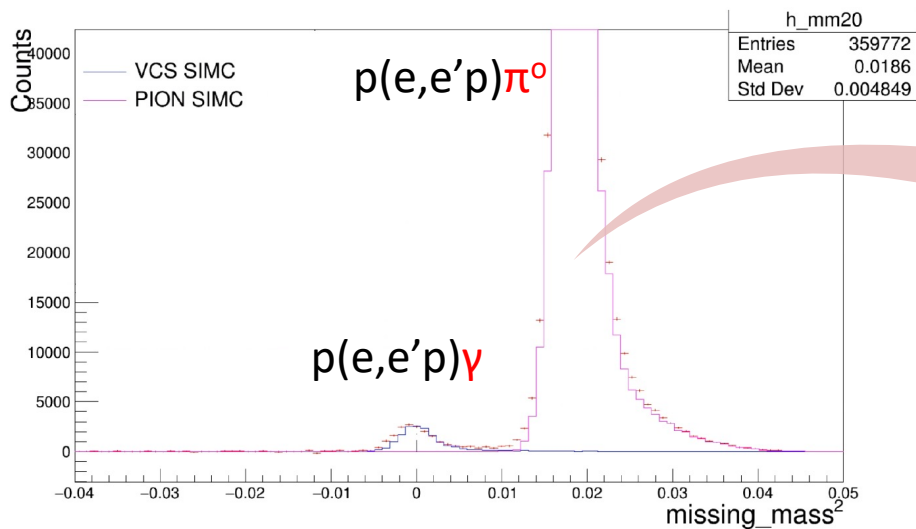


Kinematic	θ_e°	$P_e(GeV/c)$	θ_p°	$P_p(GeV/c)$
Elastic I	10.76	4.193	61.16	0.893
Elastic II	10.41	4.214	61.95	0.863
Elastic III	9.64	4.259	63.76	0.795

$p(e,e'p)\pi^0$



$N \rightarrow \Delta$ TFFs



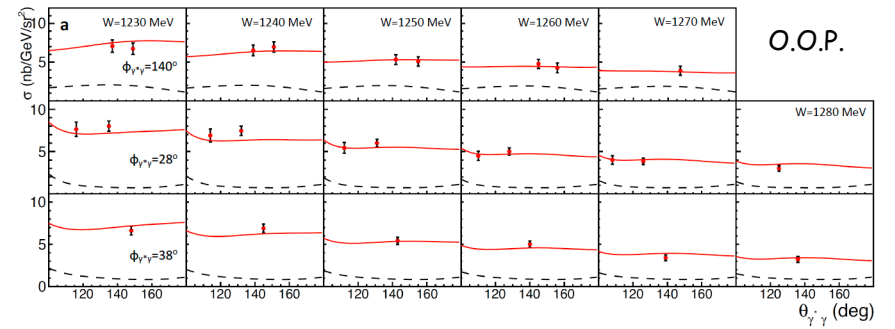
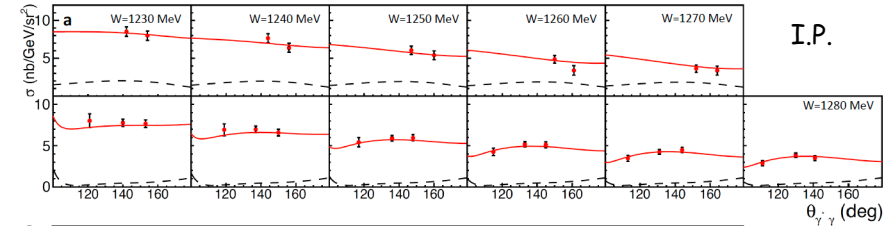
Simultaneous measurement
of the $N \rightarrow \Delta$ TFFs

TFFs well known
→ Real time normalization control

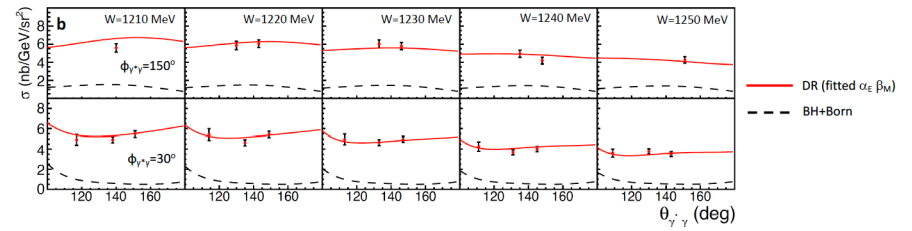
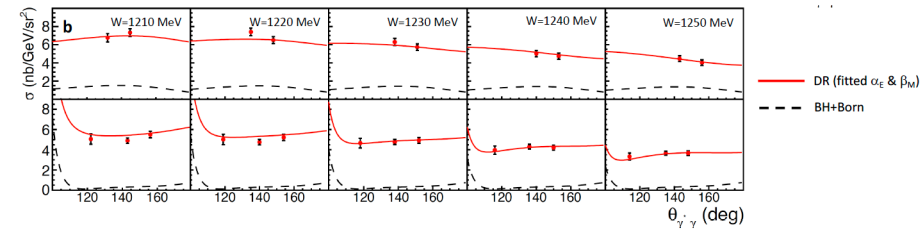
Good understanding of
spectrometer acceptance

New results: VCS cross sections

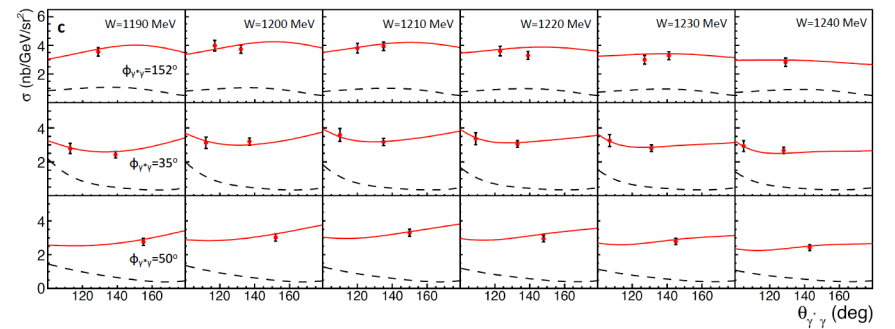
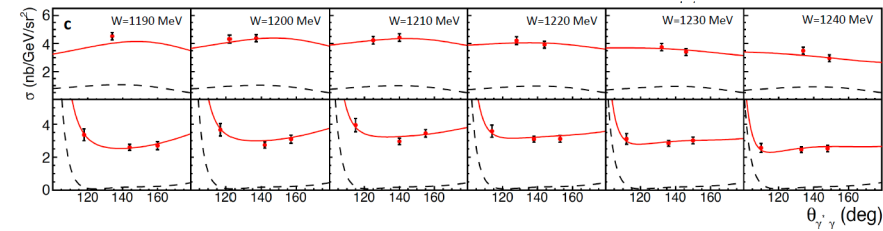
$Q^2=0.27 \text{ GeV}^2$



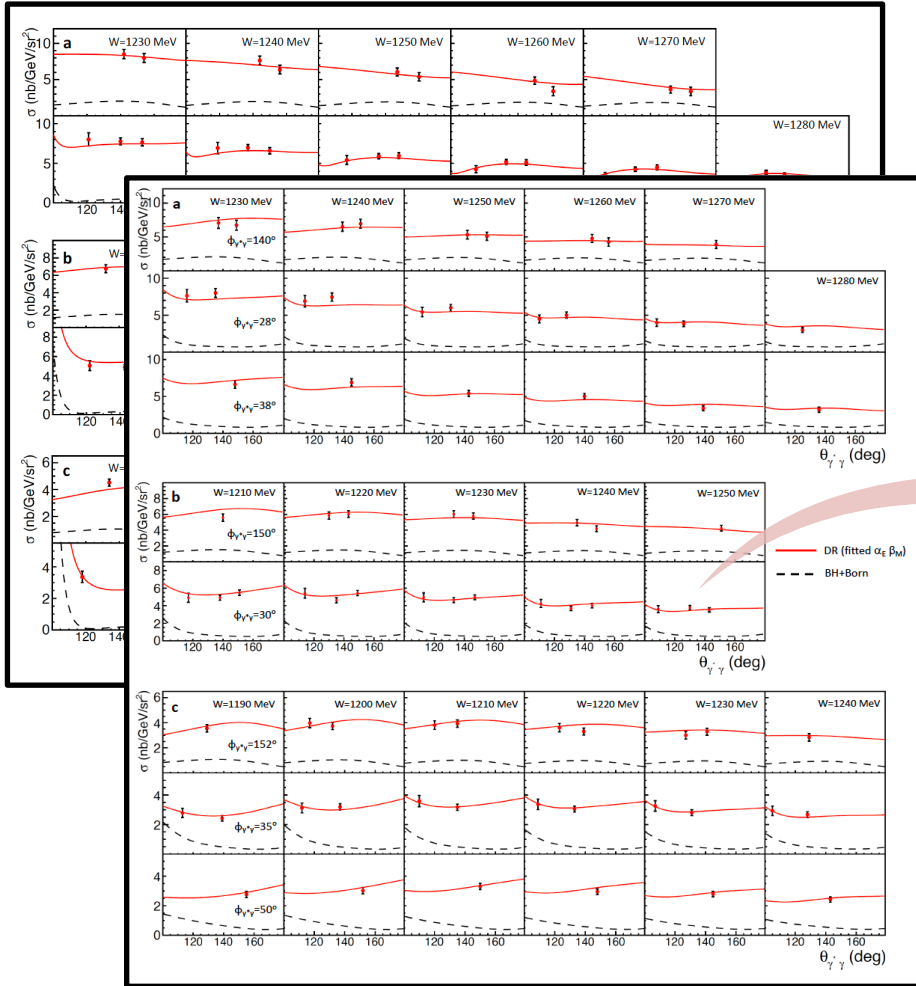
$Q^2=0.33 \text{ GeV}^2$



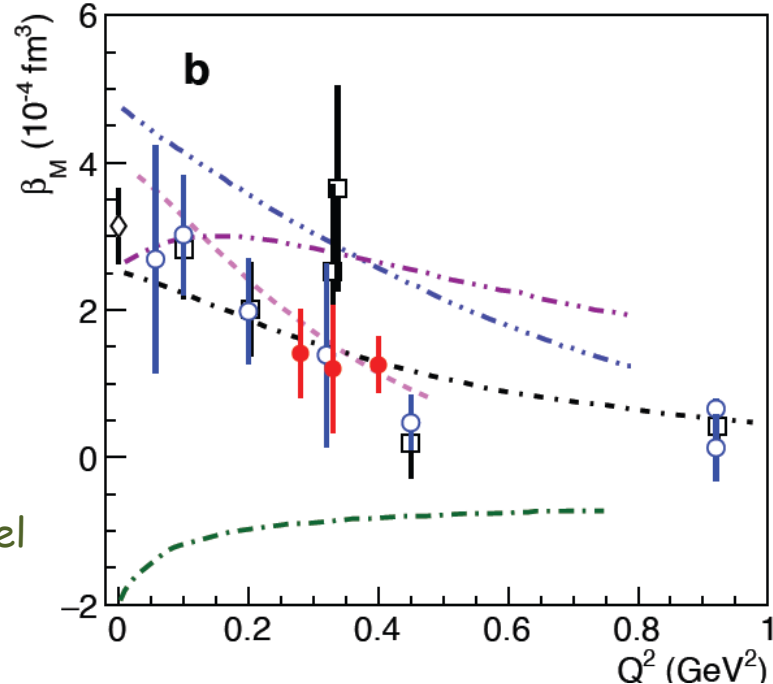
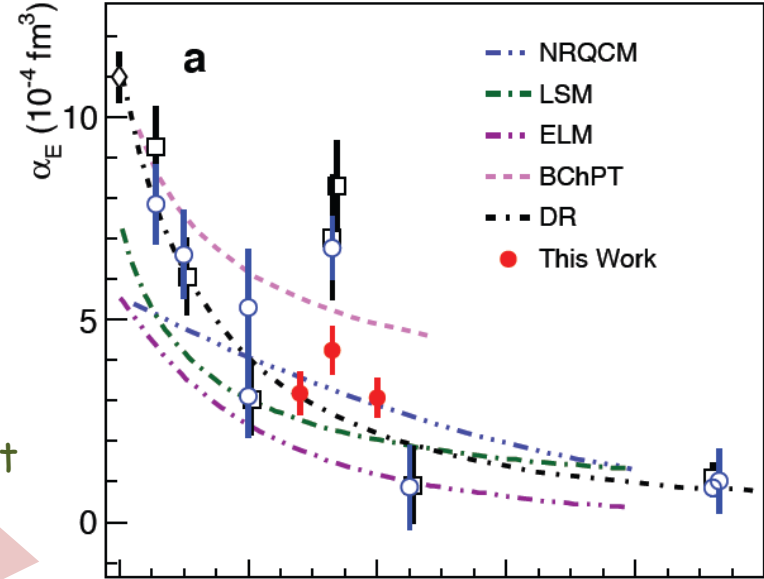
$Q^2=0.40 \text{ GeV}^2$



New results: GPs



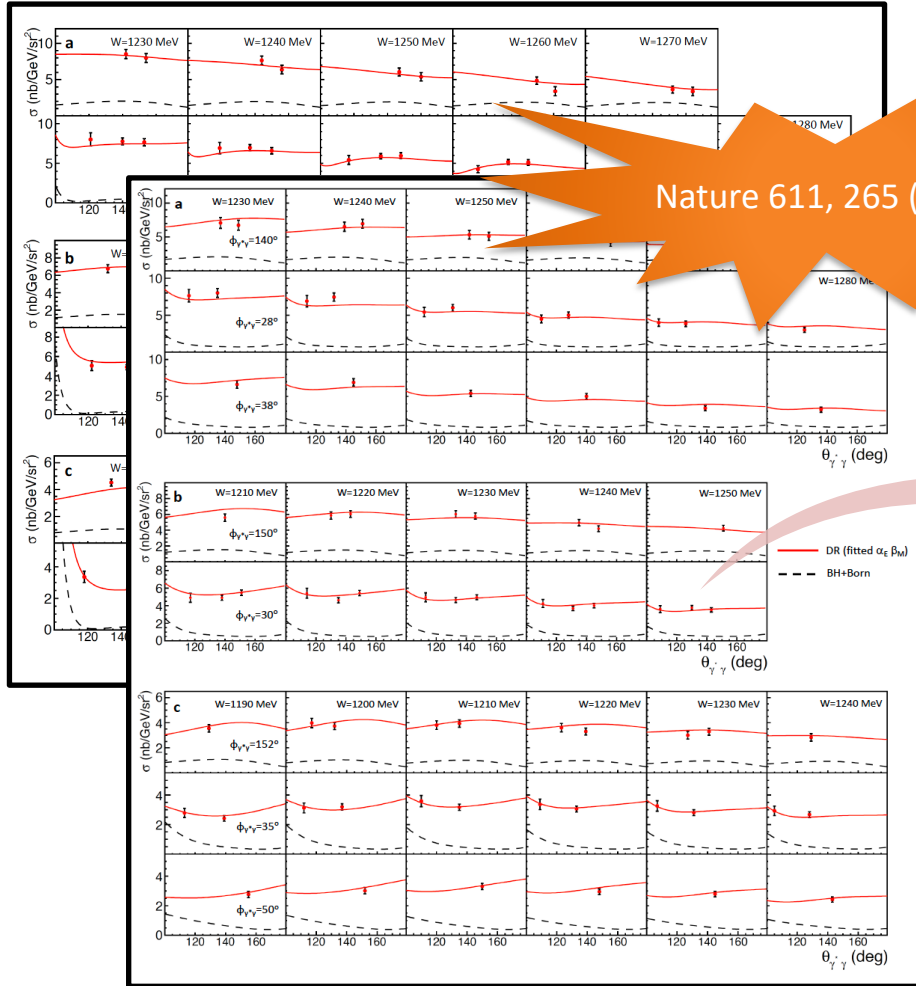
DR fit



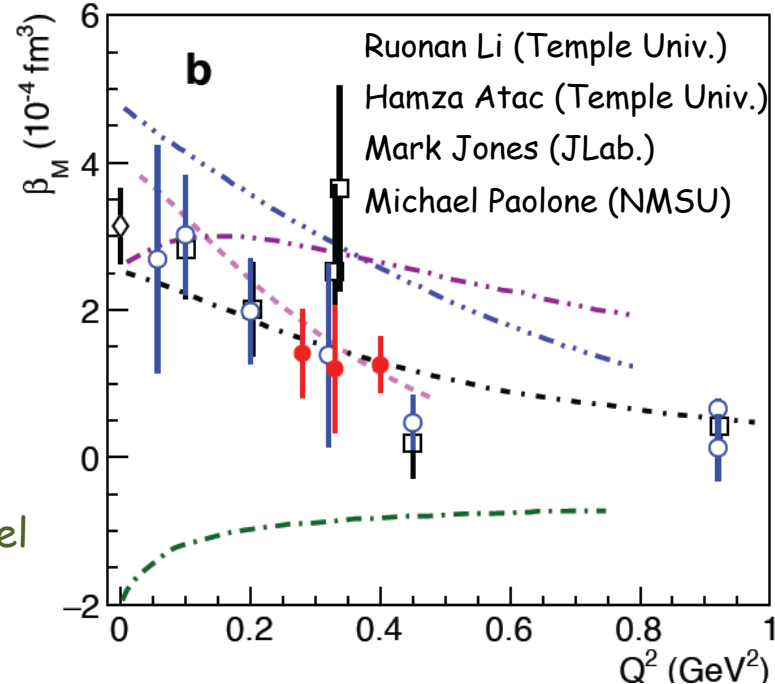
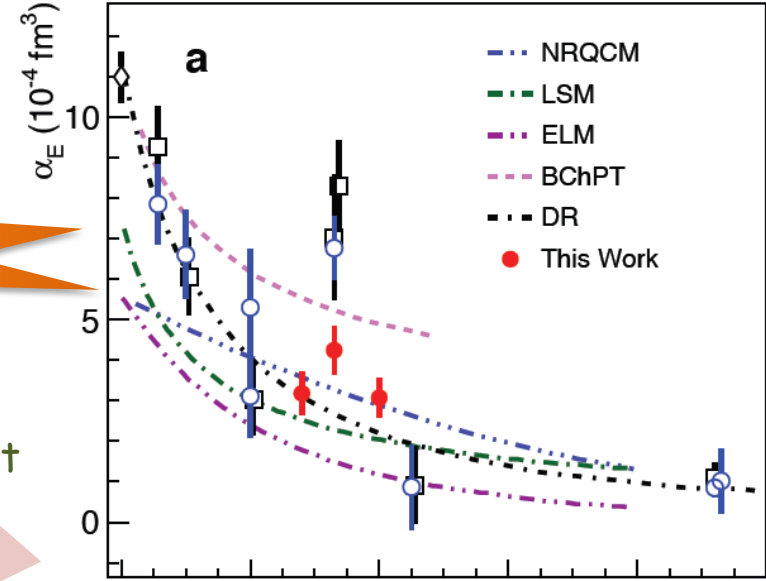
Experimental cross sections are compared to the DR model predictions for all possible values for the GPs

→ $\alpha_E(Q^2)$ and $\beta_M(Q^2)$ are fitted by a χ^2 minimization

New results: GPs



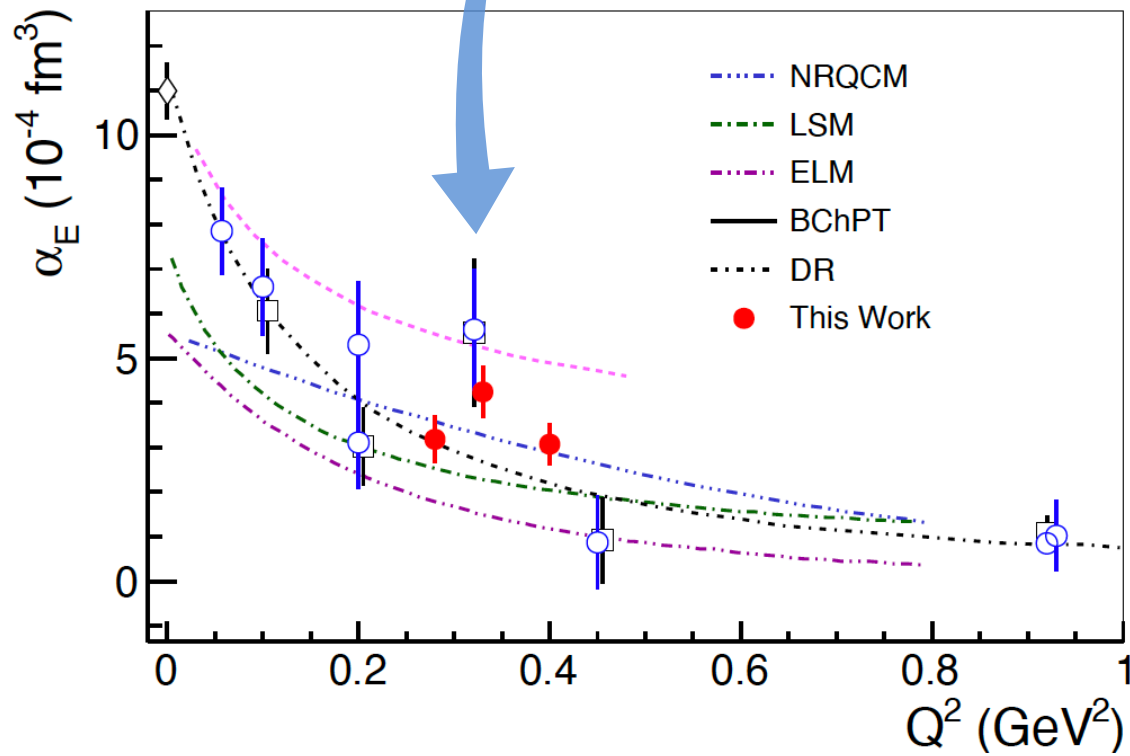
DR fit



Experimental cross sections are compared to the DR model predictions for all possible values for the GPs

→ $\alpha_E(Q^2)$ and $\beta_M(Q^2)$ are fitted by a χ^2 minimization

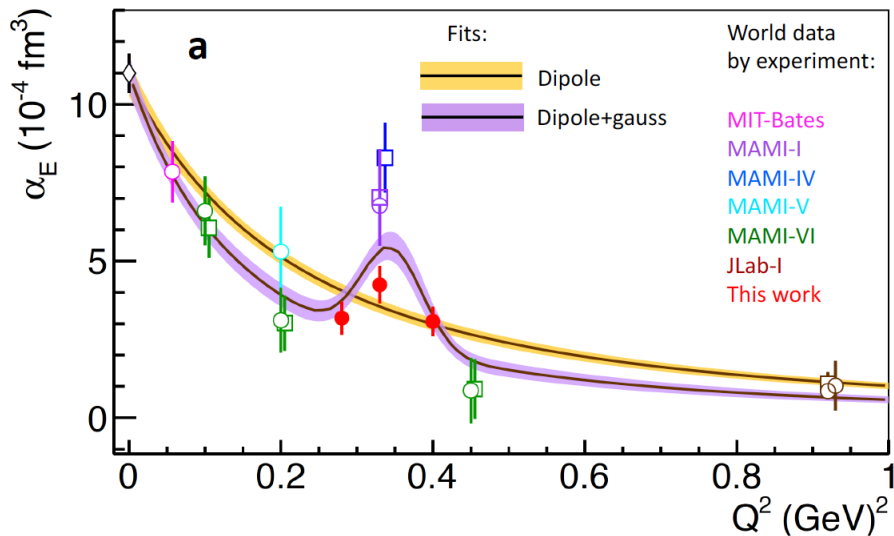
MAMI-I re-analysis (unpublished)



Is there a non-trivial structure?

Q^2 dependence of the electric GP

Traditional fits using
predefined functional forms



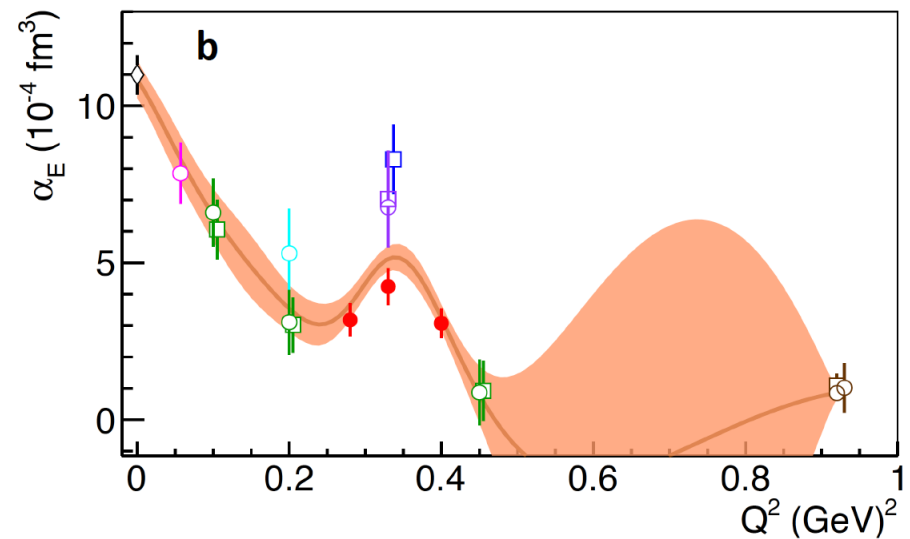
Dipole (?) ($\chi^2_v=3.7$)

Systematically overestimates MAMI-VI

Systematically underestimates MAMI-I & IV

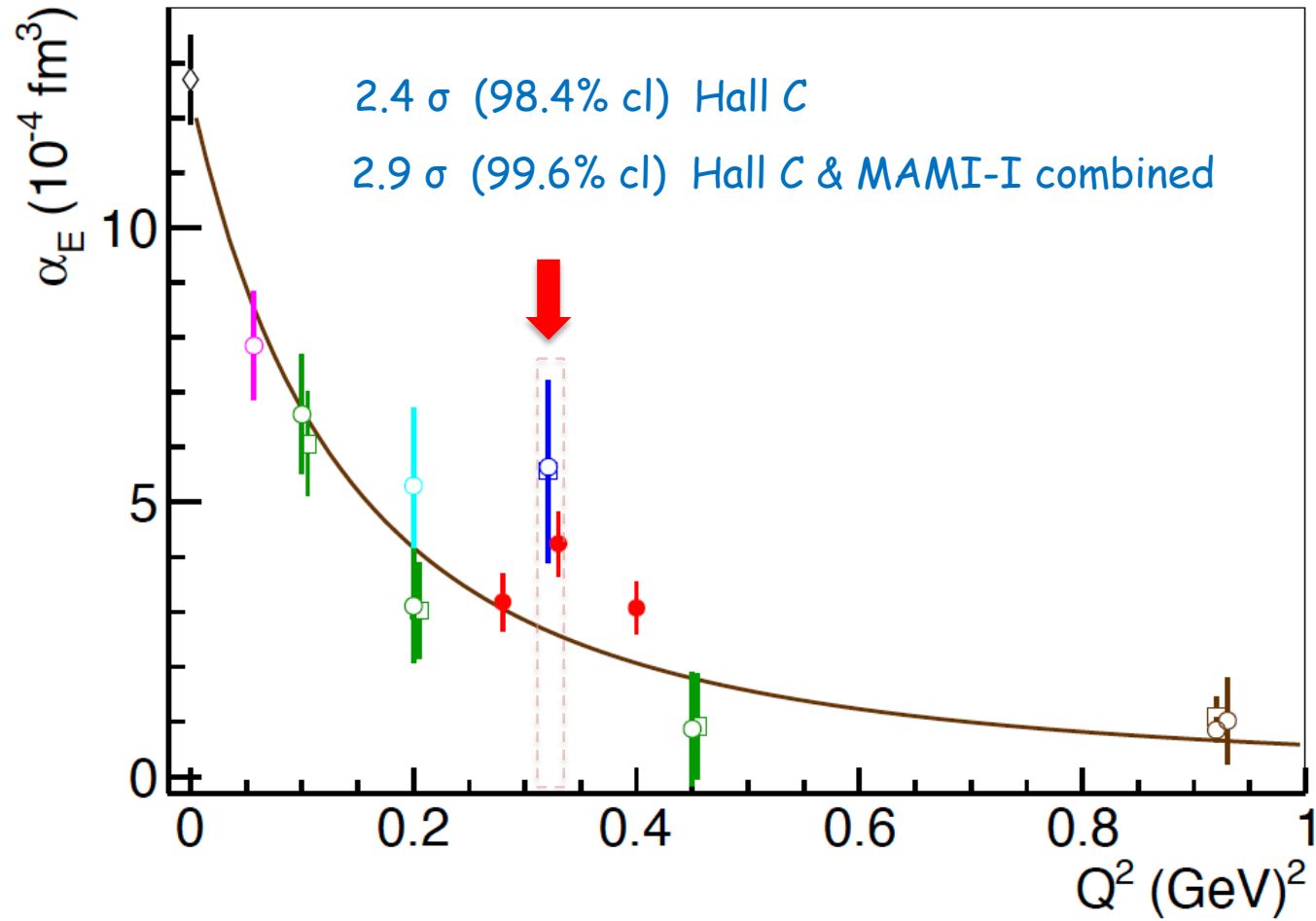
Cuts grossly through the new measurements

Data-driven techniques
no direct underlying functional
form is assumed



Rasmussen, C. E., and Williams, C. K. I. *Gaussian Processes for Machine Learning* the MIT Press, Cambridge Massachusetts, 2006, ISBN 026218253X, ©2006 Massachusetts Institute of Technology.

Deviation from a dipole fit at $Q^2 = 0.33 \text{ GeV}^2$



Theory: B χ PT

Eur. Phys. J. C (2017) 77:119
DOI 10.1140/epjc/s10052-017-4652-9

THE EUROPEAN
PHYSICAL JOURNAL C

Regular Article - Theoretical Physics


Generalized polarizabilities of the nucleon in baryon chiral perturbation theory


Vadim Lensky^{1,2,3,a}, Vladimir Pascalutsa¹, Marc Vanderhaeghen¹

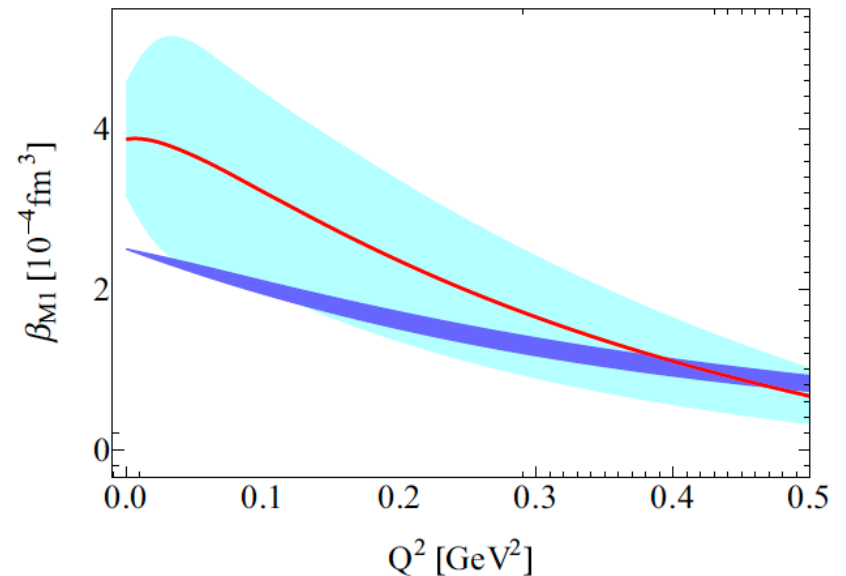
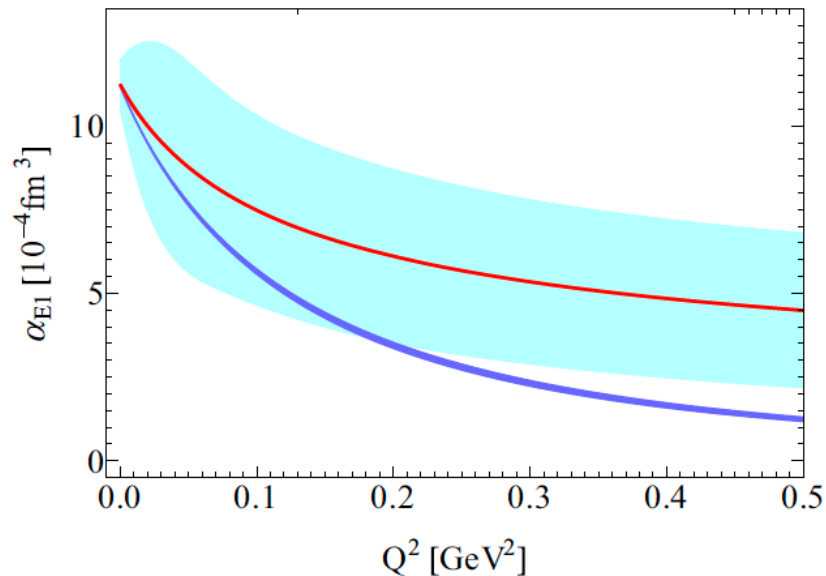
¹ Institut für Kernphysik, Cluster of Excellence PRISMA, Johannes Gutenberg Universität Mainz, 55128 Mainz, Germany

² Institute for Theoretical and Experimental Physics, Moscow 117218, Russia

³ National Research Nuclear University MEPhI (Moscow Engineering Physics Institute), Moscow 115409, Russia

 B χ PT calculation to NLO
in the δ -counting scheme

 DR calculation
D. Drechsel, B. Pasquini, M. Vanderhaeghen,
Phys. Rep. 378,99 (2003)



Theory: Lattice QCD

PHYSICAL REVIEW D **104**, 034506 (2021)

Towards charged hadron polarizabilities from four-point functions in lattice QCD

Walter Wilcox^{1,*} and Frank X. Lee^{2,†}

¹Department of Physics, Baylor University, Waco, Texas 76798, USA

²Physics Department, The George Washington University, Washington, D.C. 20052, USA

Fourier transform
of four-point CF

Measure on
the lattice

$$\alpha_E^p = \alpha \left[\frac{(1 + \kappa)^2}{4m_p^3} + \frac{T_{00}(\vec{q}_1) - T_{00}^{\text{elas}}(\vec{q}_1)}{\vec{q}_1^2} \right] \longrightarrow Q_{\mu\mu}(\vec{q}, t) = N_s^2 \sum_n |\langle h(\vec{0}) | j_\mu^L(0) | n(\vec{q}) \rangle|^2 e^{-a(E_n - m_h)t} - N_s^2 \sum_n |\langle 0 | j_\mu^L(0) | n(\vec{q}) \rangle|^2 e^{-aE_n t} \longrightarrow \alpha_E^p = \alpha \left\{ \frac{(1 + \kappa)^2}{4m_p^2} + \frac{2a}{\vec{q}_1^2} \int_0^\infty dt [Q_{00}(\vec{q}_1, t) - Q_{00}^{\text{elas}}(\vec{q}_1, t)] \right\}$$

$$Q_{\mu\mu}^{\text{elas}}(\vec{q}, t) \equiv N_s^2 |\langle h(\vec{0}) | j_\mu^L(0) | h(\vec{q}) \rangle|^2 e^{-a(E_h - m_h)t}$$

Xuan-He Wang, Xu Feng, Lu-Chuang Jin
International Symposium on Lattice Field Theory (Lattice21)

Preliminary Results on Extracting α_E

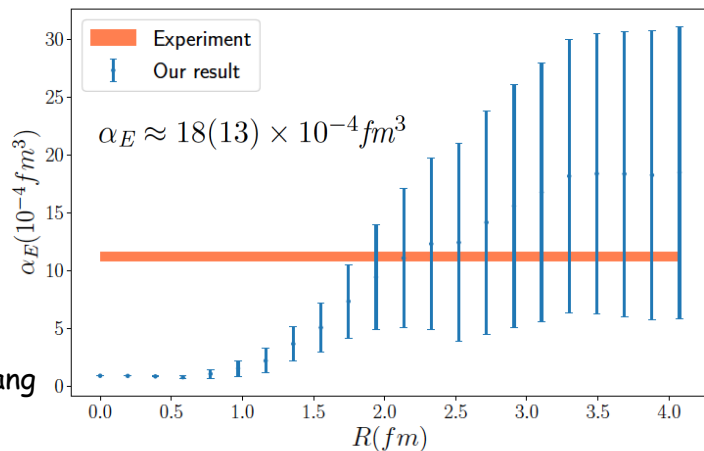


Fig.:
Lattice21, X. Wang

See talks on
Tuesday & Wednesday

Spatial dependence of induced polarizations

Nucleon form factor data → light-front quark charge densities

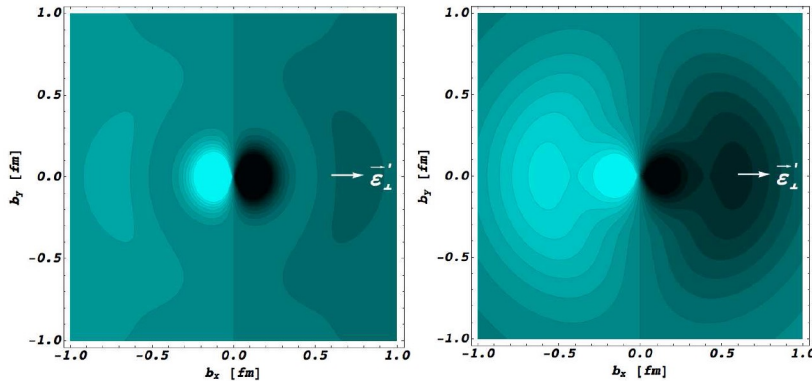
Formalism extended to the deformation of these quark densities when applying an external e.m. field:

GPs → spatial deformation of charge & magnetization densities under an applied e.m. field

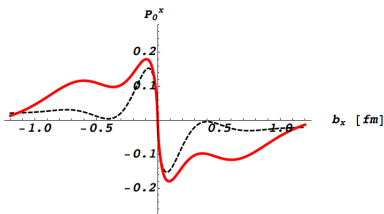
Induced polarization in a proton when submitted to an e.m. field

GP I

GP II



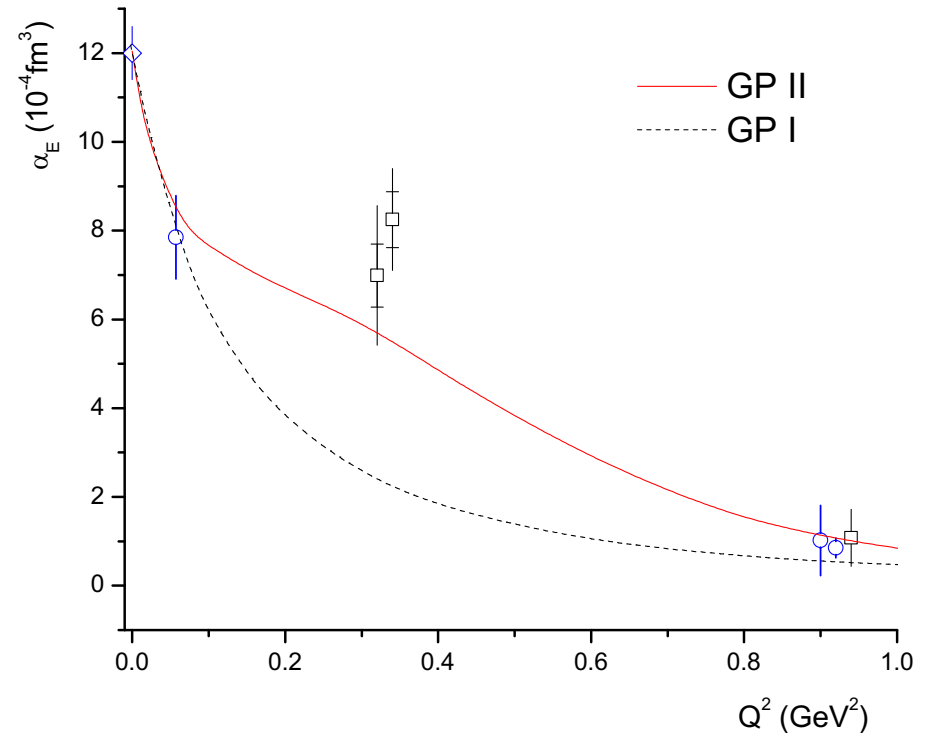
Light (dark) regions → largest (smaller) values
(photon polarization along x-axis, as indicated)



Induced polarization
along $b_y=0$

Phys. Rev. Lett. 104, 112001 (2010)

M. Gorchtein, C. Lorce, B. Pasquini, M. Vanderhaeghen

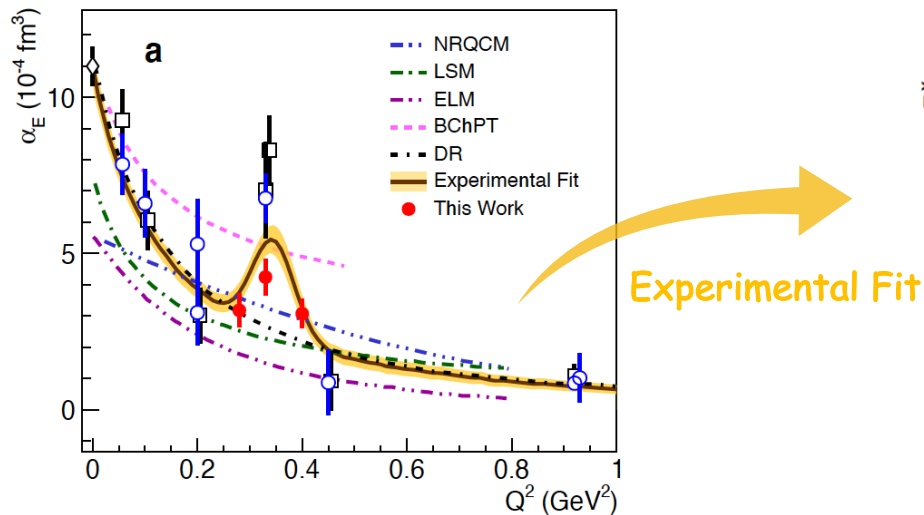


Spatial dependence of induced polarizations

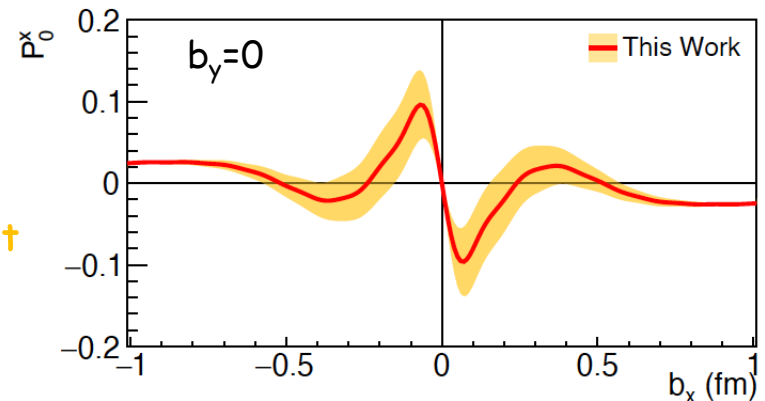
Nucleon form factor data → light-front quark charge densities

Formalism extended to the deformation of these quark densities when applying an external e.m. field:

GPs → spatial deformation of charge & magnetization densities under an applied e.m. field



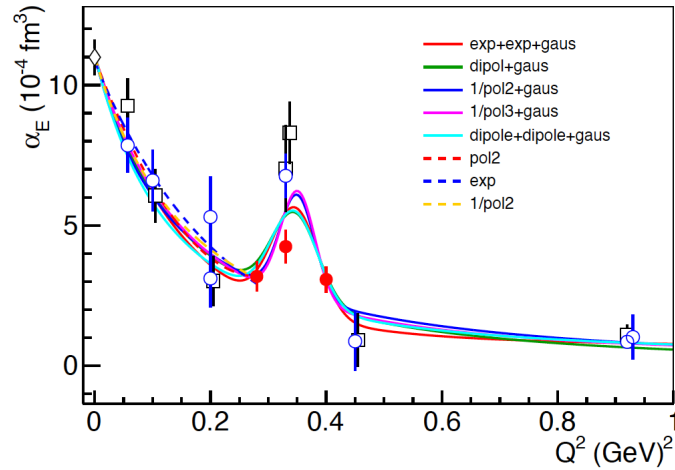
Induced polarization in a proton when submitted to an e.m. field



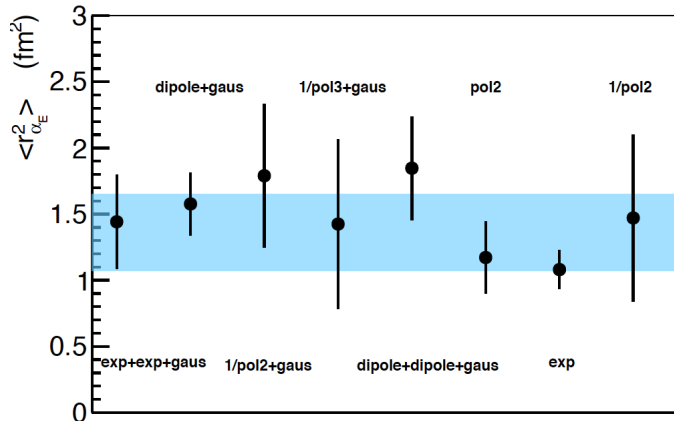
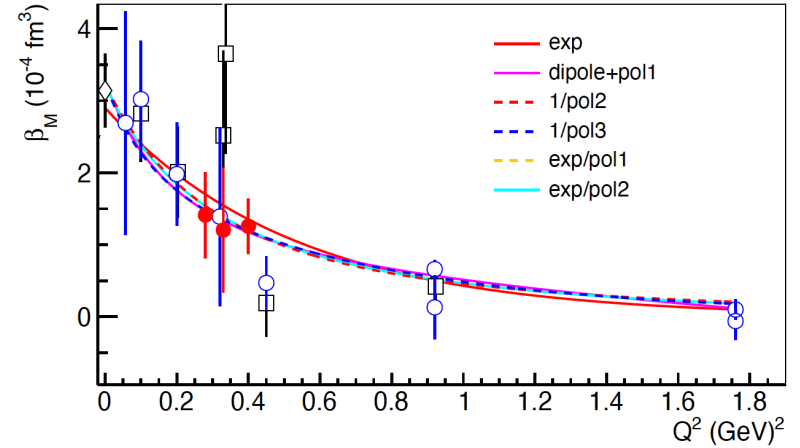
x-y defines the transverse plane with the z-axis being the direction of the fast-moving proton

Polarizability radii

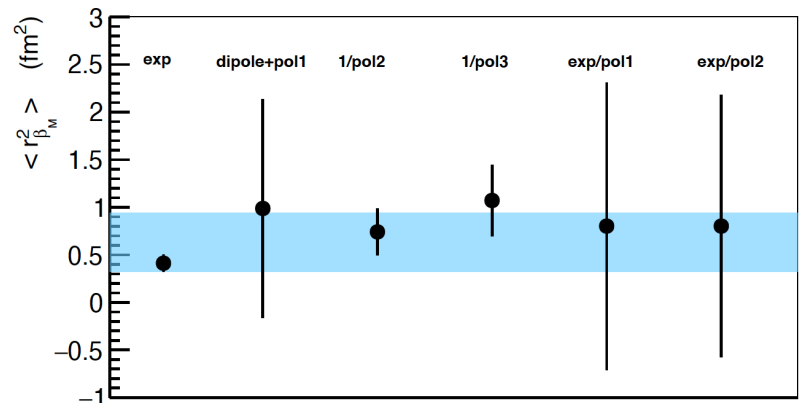
$$\langle r_{\alpha_E}^2 \rangle = \frac{-6}{\alpha_E(0)} \cdot \frac{d}{dQ^2} \alpha_E(Q^2) \Big|_{Q^2=0}$$



$$\langle r_{\beta_M}^2 \rangle = \frac{-6}{\beta_M(0)} \cdot \frac{d}{dQ^2} \beta_M(Q^2) \Big|_{Q^2=0}$$



$$\langle r_{\alpha_E}^2 \rangle = 1.36 \pm 0.29 \text{ fm}^2$$

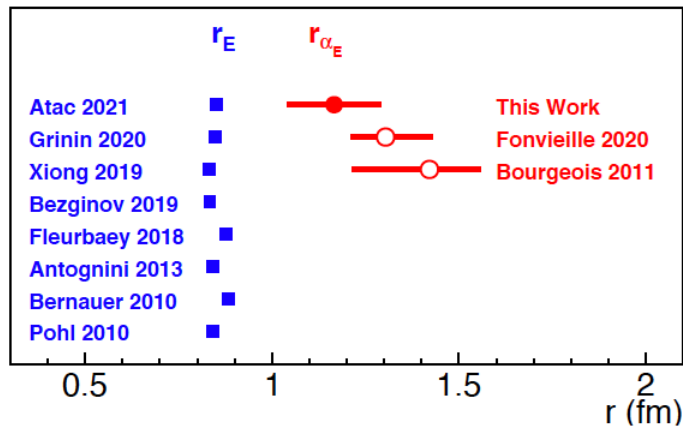
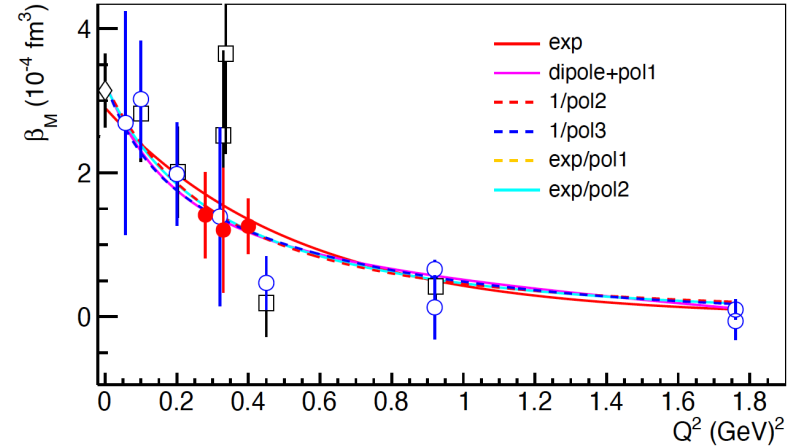
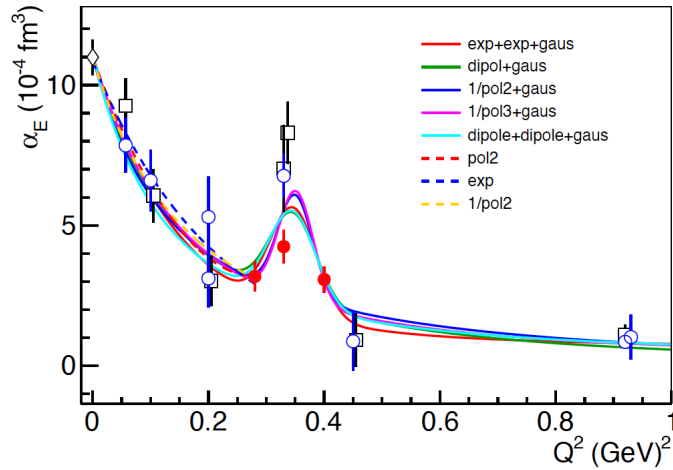


$$\langle r_{\beta_M}^2 \rangle = 0.63 \pm 0.31 \text{ fm}^2$$

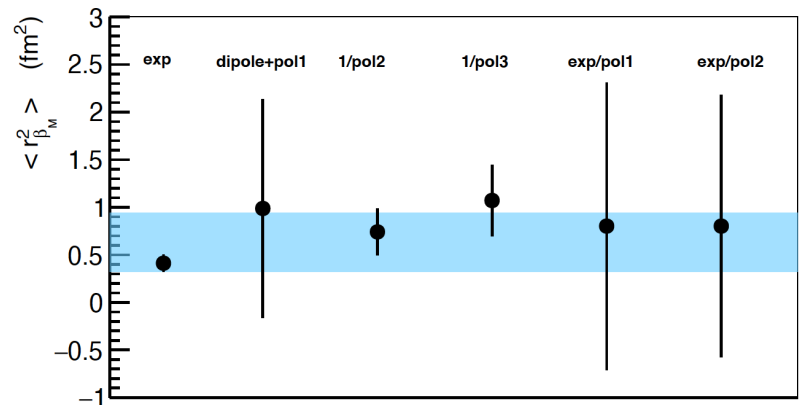
Polarizability radii

$$\langle r_{\alpha_E}^2 \rangle = \frac{-6}{\alpha_E(0)} \cdot \frac{d}{dQ^2} \alpha_E(Q^2) \Big|_{Q^2=0}$$

$$\langle r_{\beta_M}^2 \rangle = \frac{-6}{\beta_M(0)} \cdot \frac{d}{dQ^2} \beta_M(Q^2) \Big|_{Q^2=0}$$

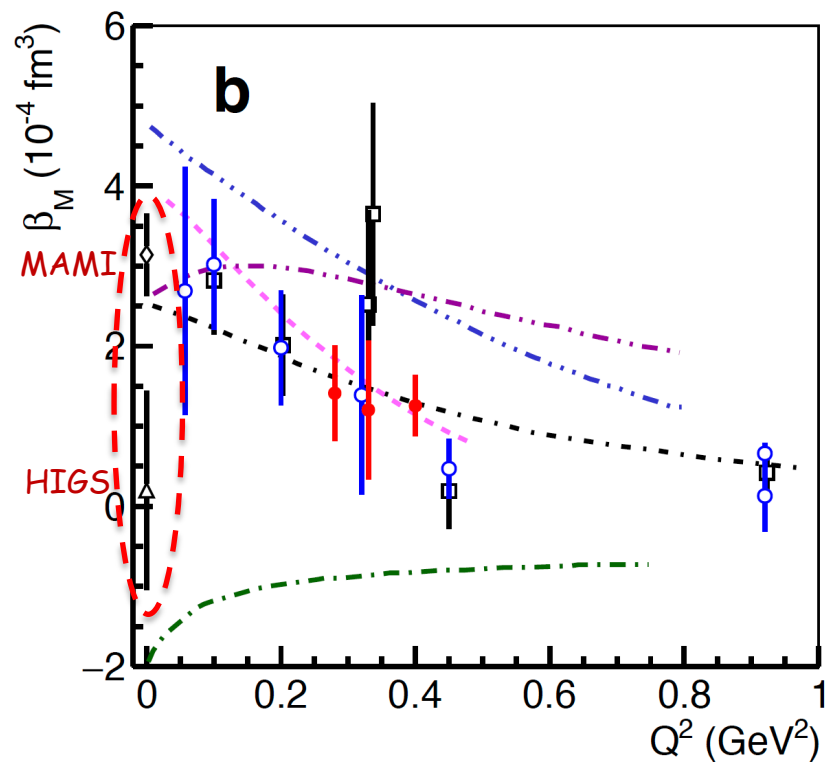
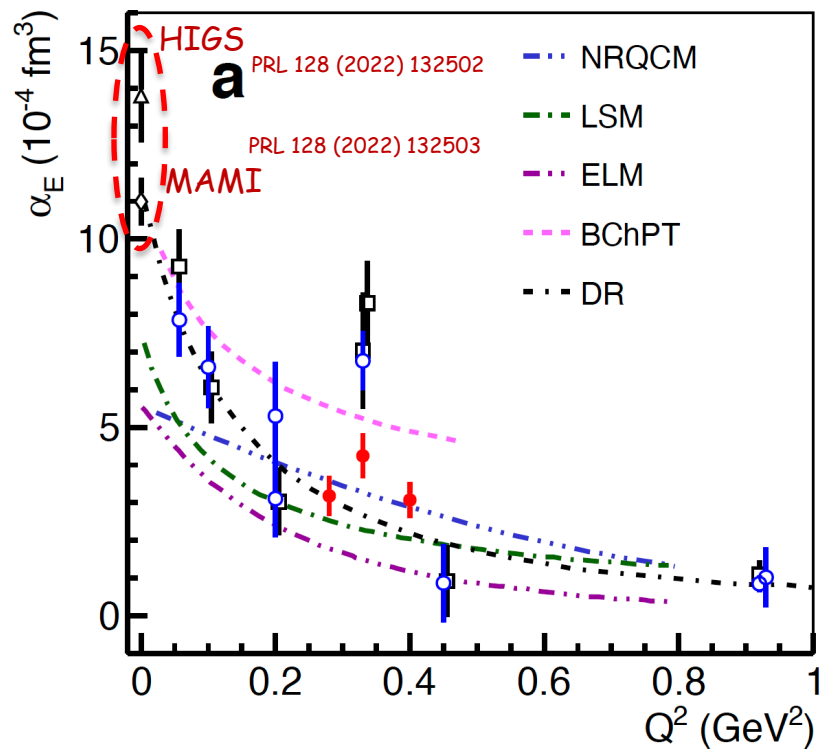


$$\langle r_{\alpha_E}^2 \rangle = 1.36 \pm 0.29 \text{ fm}^2$$

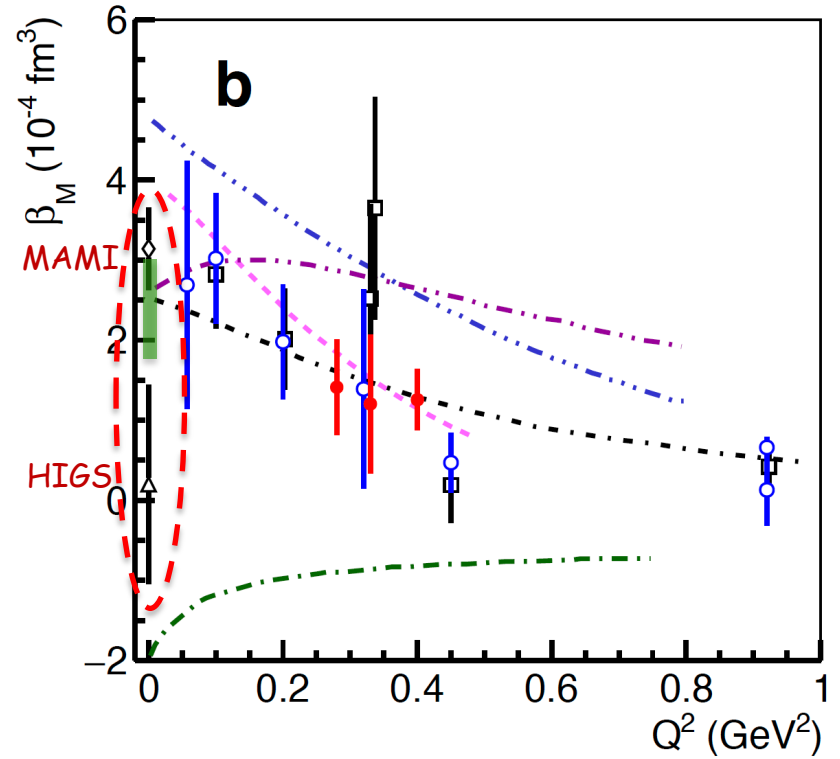
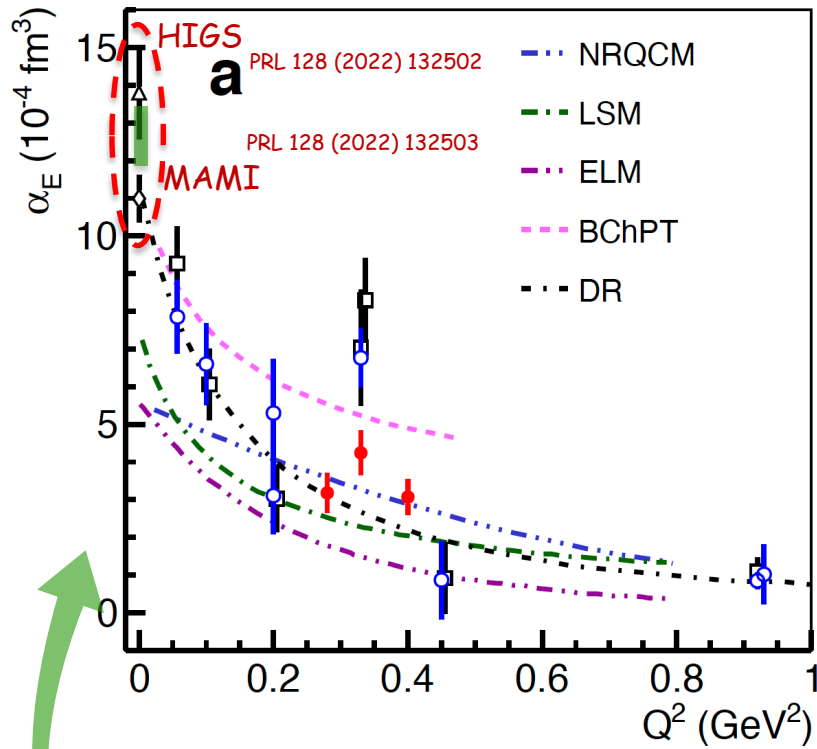


$$\langle r_{\beta_M}^2 \rangle = 0.63 \pm 0.31 \text{ fm}^2$$

Static Polarizabilities



Static Polarizabilities



PHYSICAL REVIEW LETTERS 129, 102501 (2022)

First Concurrent Extraction of the Leading-Order Scalar and Spin Proton Polarizabilities

E. Mornacchi^{1,*}, S. Rodini², B. Pasquini^{3,4} and P. Pedroni⁴

¹Institut für Kernphysik, Johannes Gutenberg-Universität Mainz, D-55099 Mainz, Germany

²Institut für Theoretische Physik, Universität Regensburg, D-93040 Regensburg, Germany

³Dipartimento di Fisica, Università degli Studi di Pavia, I-27100 Pavia, Italy

⁴INFN Sezione di Pavia, I-27100 Pavia, Italy

(Received 3 May 2022; revised 11 July 2022; accepted 2 August 2022; published 31 August 2022)

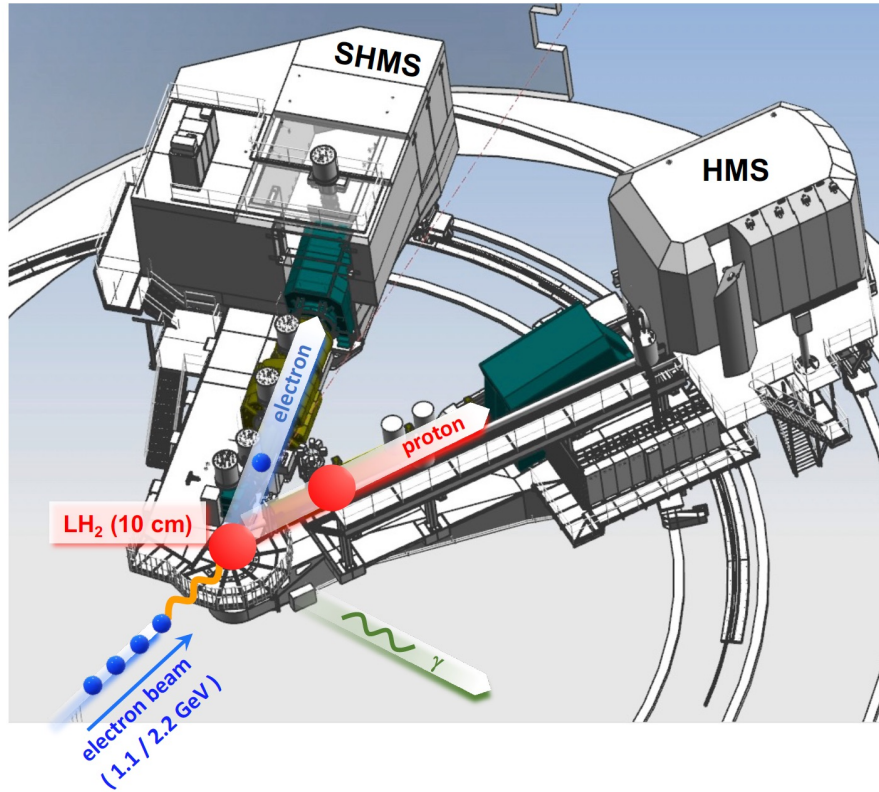
We performed the first simultaneous extraction of the six leading-order proton polarizabilities. We reached this milestone thanks to both new high-quality experimental data and an innovative bootstrap-based fitting method. These new results provide a self-consistent and fundamental benchmark for all future theoretical and experimental polarizability estimates.

$$\begin{aligned}\alpha_{E1} &= [12.7 \pm 0.8(\text{fit}) \pm 0.1(\text{model})] \times 10^{-4} \text{ fm}^3, \\ \beta_{M1} &= [2.4 \pm 0.6(\text{fit}) \pm 0.1(\text{model})] \times 10^{-4} \text{ fm}^3, \\ \gamma_{E1E1} &= [-3.0 \pm 0.6(\text{fit}) \pm 0.4(\text{model})] \times 10^{-4} \text{ fm}^4, \\ \gamma_{M1M1} &= [3.7 \pm 0.5(\text{fit}) \pm 0.1(\text{model})] \times 10^{-4} \text{ fm}^4, \\ \gamma_{E1M2} &= [-1.2 \pm 1.0(\text{fit}) \pm 0.3(\text{model})] \times 10^{-4} \text{ fm}^4, \\ \gamma_{M1E2} &= [2.0 \pm 0.7(\text{fit}) \pm 0.4(\text{model})] \times 10^{-4} \text{ fm}^4,\end{aligned}$$

Moving Forward

VCS-II

New JLab proposal for PAC51 (summer 2023)

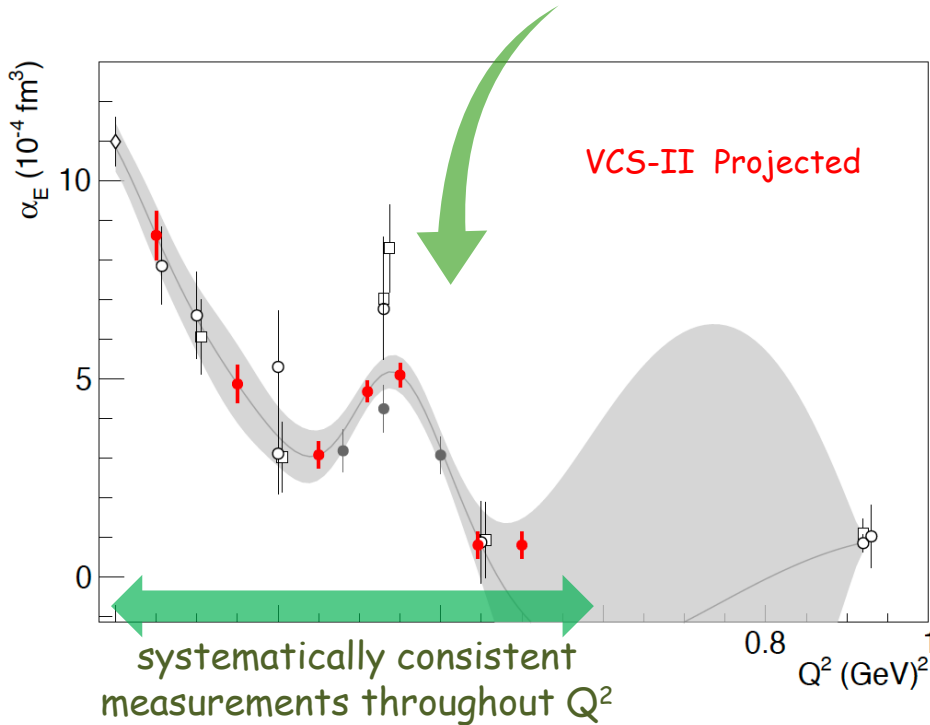


$E_0 = 1.1 \text{ \& } 2.2 \text{ GeV}$ and 60 days of beamtime

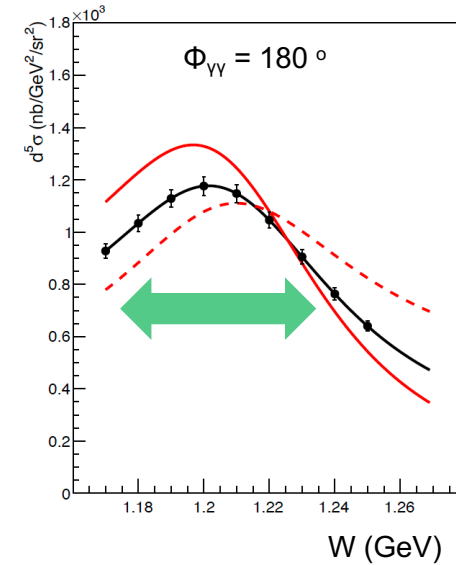
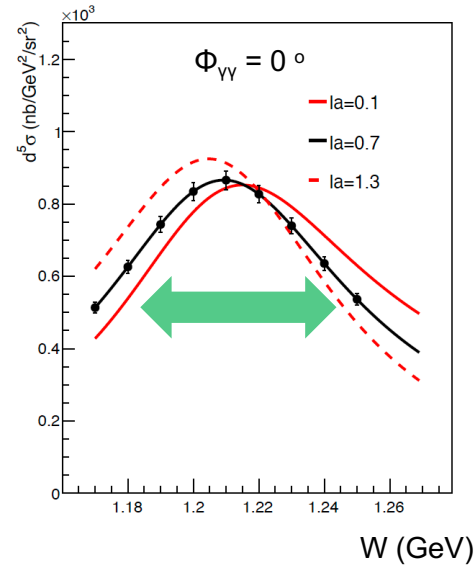
Kinematic Group	Kinematic Setting	$\theta_{\gamma^* \gamma}^\circ$	θ_e°	$P'_e(\text{MeV}/c)$	θ_p°	$P'_p(\text{MeV}/c)$	$I (\mu\text{A})$	beam time (days)
GI	Kin I	110	14.3	736.3	54.45	493.93	15	1.00
	Kin II	133	14.3	736.3	44.93	556.10	15	1.00
	Kin IIIa	147	14.3	736.3	11.26	583.05	15	1.00
	Kin IIIb	147	14.3	736.3	39.06	583.05	15	1.00
	Kin IVa	160	14.3	736.3	16.73	599.95	15	1.00
	Kin IVb	160	14.3	736.3	33.59	599.95	15	1.00
GII	Kin I	115	11.22	1783.0	15.33	615.69	10	1.50
	Kin IIa	125	11.22	1783.0	56.54	647.85	10	2.50
	Kin IIb	125	11.22	1783.0	18.60	647.85	10	1.50
	Kin IIIa	145	11.22	1783.0	49.77	697.99	10	1.50
	Kin IIIb	145	11.22	1783.0	25.37	697.99	10	1.00
	Kin IVa	165	11.22	1783.0	42.82	726.87	10	1.00
	Kin IVb	165	11.22	1783.0	32.32	726.87	10	1.00
GIII	Kin I	115	14.73	1729.7	20.58	706.89	30	1.75
	Kin IIa	130	14.73	1729.7	54.89	758.24	30	2.00
	Kin IIb	130	14.73	1729.7	24.78	758.24	30	1.75
	Kin IIIa	150	14.73	1729.7	48.99	808.24	30	1.75
	Kin IIIb	150	14.73	1729.7	30.68	808.24	30	1.75
	Kin IVa	170	14.73	1729.7	42.90	834.12	30	1.00
	Kin IVb	170	14.73	1729.7	36.76	834.12	30	1.00
GIV	Kin I	100	16.32	1749.3	23.83	664.52	35	1.75
	Kin II	120	16.32	1749.3	28.01	738.39	50	1.25
	Kin IIIa	140	16.32	1749.3	32.84	795.37	70	1.00
	Kin IIIb	140	16.32	1749.3	53.80	795.37	70	2.00
	Kin IVa	155	16.32	1749.3	36.69	824.46	70	1.50
	Kin IVb	155	16.32	1749.3	49.95	824.46	70	2.50
GV	Kin Va	170	16.32	1749.3	40.66	840.48	70	1.00
	Kin Vb	170	16.32	1749.3	45.99	840.48	70	1.00
	Kin I	100	17.72	1676.41	19.75	723.69	35	2.00
	Kin II	120	17.72	1676.41	24.25	808.93	50	1.50
	Kin IIIa	140	17.72	1676.41	29.34	874.74	70	1.50
	Kin IIIb	140	17.72	1676.41	51.12	874.74	70	2.00
GVI	Kin IVa	155	17.72	1676.41	33.36	908.37	70	2.00
	Kin IVb	155	17.72	1676.41	47.10	908.37	70	2.00
	Kin Va	170	17.72	1676.41	37.47	926.91	70	1.00
	Kin Vb	170	17.72	1676.41	42.99	926.91	70	1.00
	Kin I	120	20.45	1623.1	25.31	886.59	75	1.00
	Kin IIa	140	20.45	1623.1	29.91	956.82	75	1.00
GVI	Kin IIb	140	20.45	1623.1	49.81	956.82	75	1.50
	Kin IIIa	155	20.45	1623.1	33.58	992.83	75	1.50
	Kin IIIb	155	20.45	1623.1	46.14	992.83	75	2.00

VCS-II Projected Measurements

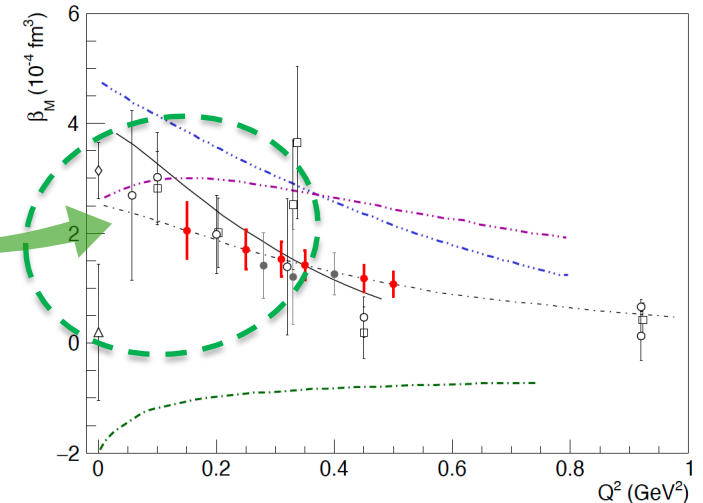
High precision measurements
combined with a fine mapping in Q^2



Targeted measurements to fully
exploit the sensitivity to the GPs



Improve upon β_M :
Pin down the competing
para/dia-magnetic contributions
in the nucleon



Measuring with positrons

Positrons allow for an independent path to access experimentally the GPs

Eur. Phys. J. A 57 (2021) 11, 316

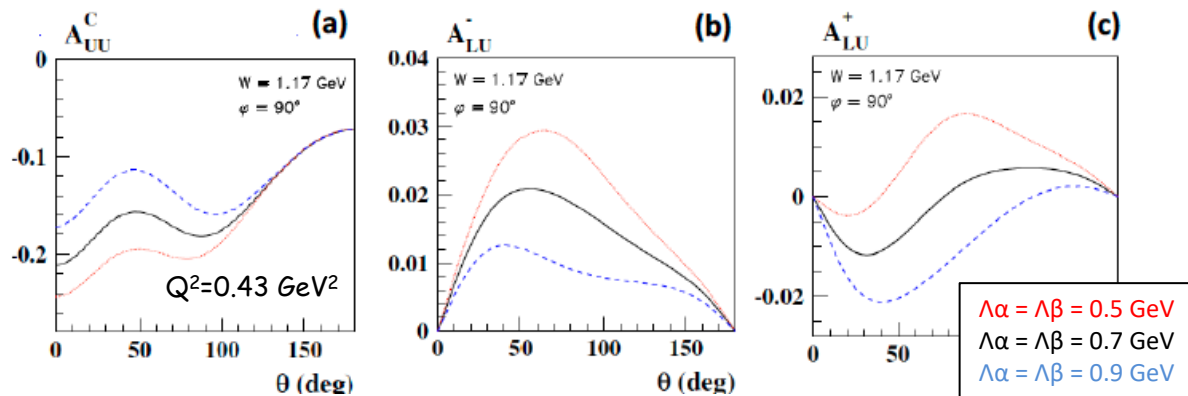
Virtual Compton scattering at low energies with a positron beam

Barbara Pasquini^{a,1,2}, Marc Vanderhaeghen^{b,3}

¹Dipartimento di Fisica, Università degli Studi di Pavia, 27100 Pavia, Italy

²Istituto Nazionale di Fisica Nucleare, Sezione di Pavia, 27100 Pavia, Italy

³Institut für Kernphysik and PRISMA⁺ Cluster of Excellence, Johannes Gutenberg Universität, D-55099 Mainz, Germany



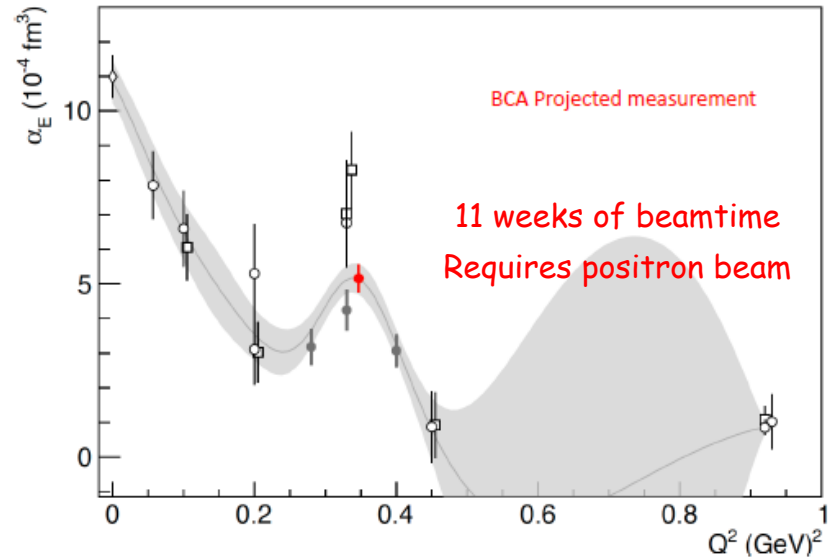
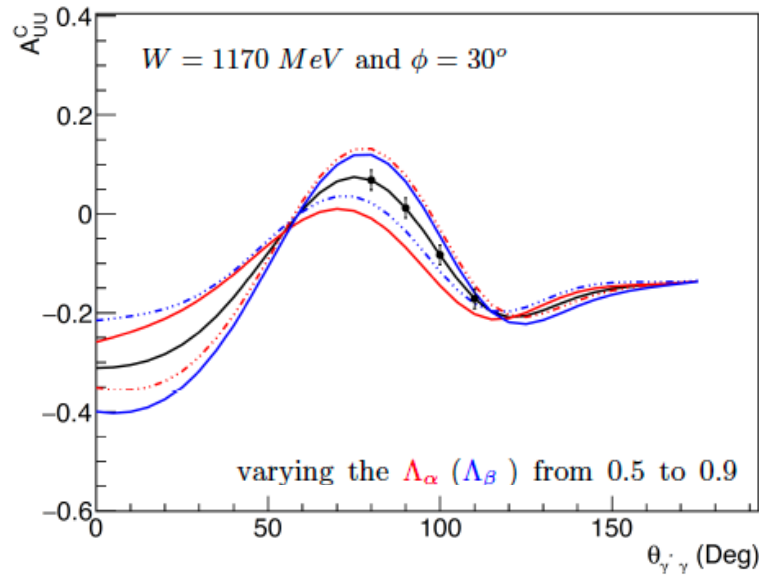
(a): The beam-charge asymmetry as a function of the photon scattering angle at $Q^2 = 0.43 \text{ GeV}^2$.

(b) & (c): The electron and positron beam-spin asymmetry as a function of the photon scattering angle for out-of-plane kinematics.

Unpolarized beam charge asymmetry (BCA):
$$A_{UU}^C = \frac{(d\sigma_+^+ + d\sigma_-^+) - (d\sigma_+^- + d\sigma_-^-)}{d\sigma_+^+ + d\sigma_-^+ + d\sigma_+^- + d\sigma_-^-}$$

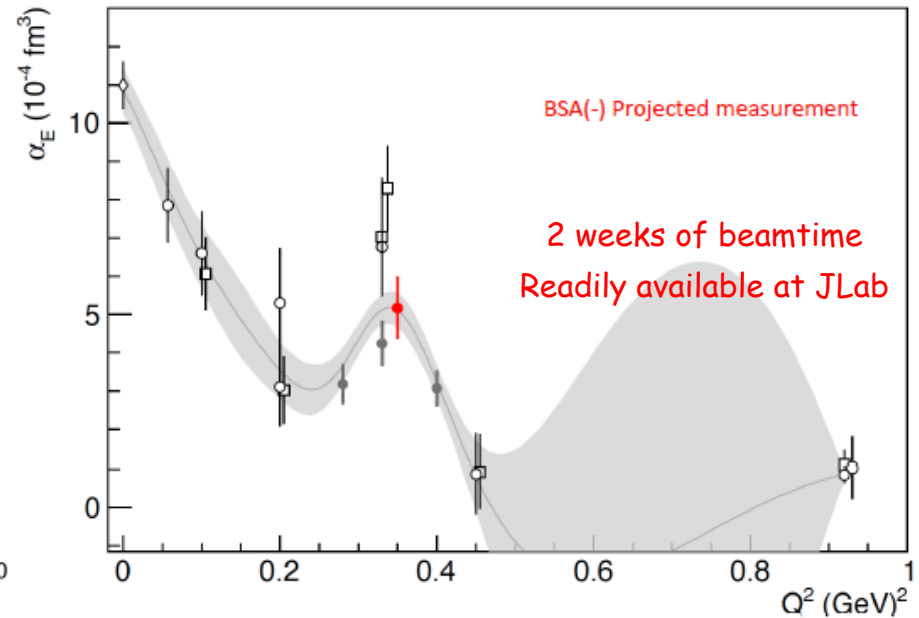
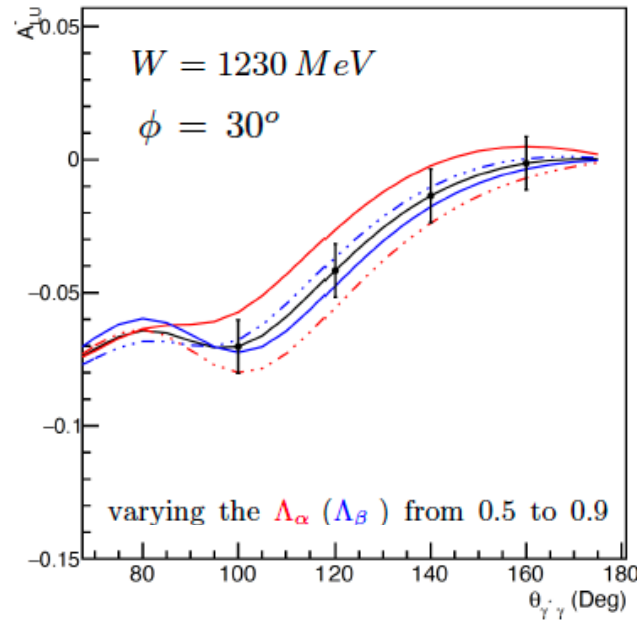
Lepton beam spin asymmetry (BSA):
$$A_{LU}^e = \frac{d\sigma_+^e - d\sigma_-^e}{d\sigma_+^e + d\sigma_-^e}$$

BCA



Hall C (SHMS / HMS) { e^- : ~ 1 week of beamtime @ 50 μA
and
 e^+ : ~ 10 weeks of beamtime @ 5 μA

BSA



Hall C (SHMS / HMS) { e^- (pol. 85% @ 70 μA) : ~ 2 weeks of beamtime
 or
 e^+ (pol. 60% @ 50 nA) : ~ 3 orders of magnitude more beamtime

Measurement of the Generalized Polarizabilities of the Proton
 with positron and polarized electron beams

Letter of Intent to Jefferson Lab PAC-51

Summary

Progress in the study of fundamental system properties that characterize the proton's response to an EM field

Insight to spatial deformation of the nucleon densities under an applied EM field, interplay of para/dia-magnetic mechanisms in the proton, polarizability radii, ...

Electric GP: $\left\{ \begin{array}{l} \text{possibility for a non-trivial (non-monotonic) behavior in } a_E(Q^2) \\ \text{(albeit with a smaller magnitude than originally suggested)} \\ \text{or} \\ \text{at minimum: strong tension between world data} \end{array} \right.$

Strong constraints to theoretical predictions (we can improve further)

High precision benchmark data for theory & upcoming LQCD calculations

Future measurements:

Pinn down with precision the shape of the a_E structure (if it exists) - important input for the theory

Measure via a different channel (positrons)

Thank you!